Durham E-Theses

Space charge limited currents in Cadmium Sulphide

Marlor, G. A.

How to cite:

Marlor, G. A. (1962) *Space charge limited currents in Cadmium Sulphide*, Durham theses, Durham University. Available at Durham E-Theses Online: http://etheses.dur.ac.uk/10091/

Use policy

The full-text may be used and/or reproduced, and given to third parties in any format or medium, without prior permission or charge, for personal research or study, educational, or not-for-profit purposes provided that:

- a full bibliographic reference is made to the original source
- a link is made to the metadata record in Durham E-Theses
- the full-text is not changed in any way

The full-text must not be sold in any format or medium without the formal permission of the copyright holders.

Please consult the full Durham E-Theses policy for further details.

Academic Support Office, The Palatine Centre, Durham University, Stockton Road, Durham, DH1 3LE
e-mail: e-theses.admin@durham.ac.uk Tel: +44 0191 334 6107
http://etheses.dur.ac.uk

Space Charge Limited Currents in Cadmium Sulphide

by

G. A. Marlor B.Sc.

Presented in canditure for the degree of Master of Science of the University of Durham.

September 1962

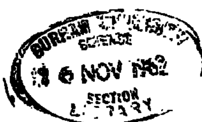

Introduction

Cadmium sulphide has been extensively studied for a number of years. The chief interest has been centred on the photoconductive properties of sintered layers and single crystals. The present work is concerned with a closely allied topic, the injection of current carriers in excess of those present in thermal equilibrium in single crystals. The conduction due to these excess carriers is closely linked to the conduction due to excess carriers provided by optical excitation, since excess carriers are subject to similar influences which ever way they are produced. No measurements of the photoconductive properties of cadmium sulphide are included, but where relevant they are discussed for completeness.

The first chapter considers the basic problems of conduction by injected carriers, where ideally conduction is only limited by the space charge of the injected carriers. The next two chapters review the pertinent experimental and theoretical work previously carried out.

Chapter four deals with the preparation of single crystals of cadmium sulphide and includes an account of the techniques used in our laboratory.

The remaining three chapters deal with the experiments carried out, their analysis and the conclusions that can be

drawn. The experiments consist of a series of current versus voltage measurements, under different conditions, and the observation and measurement of luminescence from the crystals. Measurements of the current through crystals when pulsed voltages were applied have disclosed two interesting discontinuities in the current. A preliminary investigation of these phenomena is described, and tentative explanations of the discontinuities put forward.

Throughout this work the emphasis is on understanding the physics of the various processes. Once a better understanding of the problems involved in space charge limited conduction is gained, considerable exploitation should be possible. For example, since the forbidden gap width is large, devices could operate at higher temperatures than conventional semiconductor devices. This is of considerable interest from an applications point of view.

In the present work, space charge effects are used to investigate the properties of cadmium sulphide. As with most semiconductor problems, the chief difficulties stem from the number and complexity of the imperfections in the crystals. Further progress will certainly be made if the imperfections in cadmium sulphide crystals can be reduced.

Acknowledgments

The author wishes to thank C.V.D. Admiralty for the financial assistance that made this work possible. He is indebted to Professor D. A. Wright for the use of his laboratory facilities; to Dr. J. Woods for his supervision and unfailing guidance; to Miss R. Noble for her assistance in the preparation of single crystals, many luminescence observations and for her assistance in preparing the enclosed figures; and to the Technical Staff of the Department of Applied Physics headed by F. Spence.

Contents

		Page
Chapter I	General Introduction	
1.1	Electron energy levels in crystalline solids	1
1.2	Metals, insulators and semiconductors	2
1.3	Effective mass of electrons	4
1.4	Concept of mobility	5
1.5	The Fermi level	5
1.6	Density of states and carrier distribution	6
1.7	Conduction mechanisms in insulators	8
1.8	Analysis of Mott and Gurney	9
1.9	Modified Analysis - Thermionic Analogy	14
1.10	Contact Limitations	15
1.11	Levels in the Forbidden Gap	18
1.12	Summary	20
Chapter II	Previous Experimental Evidence	
2.1	Properties of Cadmium Sulphide	22
2.2	The Metal-Insulator Contact	24
2.3	Hole injection	27
2.4	Experimental Evidence for Space Charge Limited Conduction	28
2.5	Evidence for two carrier S.C.L. conduction in Cadmium Sulphide	31
2.6	Object of the Research	32
2.7	Recent work by Ruppel	33
2.8	Recent work by Bube	34

		Page
Chapter III	Theoretical Work	
3.1	Basis of Lampert's Theory	35
3.2	The Limiting Characteristics	36
3.3	Results of Lampert's Analysis	38
3.4	Two-carrier space charge limited conduction in trap free insulators	41
3.5	Extensions of Lampert and Rose	42
3.6	Photoconductivity in the Gain-Bandwidth product	45
3.7	Contact controlled response time	47
Chapter IV	Preparation of Single Crystals of Cadmium Sulphide	
4.1	Summary of methods of growth from the vapour phase.	49
4.2	Preparation by combination of the elements	50
4.3	Preparation by iodine transport	51
4.4	Preparation by sublimation of the compound	52
4.5	General observations on the sublimation growth of cadmium sulphide	53
4.6	Conclusions	54
Chapter V	Apparatus, experimental procedures and results	
5.1	Contact materials and methods of application	56
5.2	Direct current-voltage characteristics at room temperature	57
5.3	Temperature variation of direct current-voltage characteristic	60
5.4	Current-voltage characteristics using pulsed fields	62

		Page
5.5	Direct current luminescence	66
5.6	Pulsed current luminescence	70
Chapter VI	Discussion of results	
6.1	Effect of contacts	73
6.2	Direct current-voltage characteristics at room temperature	76
6.3	The temperature variation of the direct current-voltage characteristics	79
6.4	Current-voltage characteristics using pulsed fields	83
6.5	Analysis of direct current luminescence	85
6.6	Pulsed current luminescence	86
Chapter VII	Conclusions	
7.1	Crystal growth	89
7.2	Contact to cadmium sulphide	89
7.3	Single carrier space charge limited conduction	89
7.4	Two carrier space charge limited conduction	90

Space Charge Limited Currents in Cadmium Sulphide

Chapter I General Introduction

1.1 Electron energy levels in crystalline solids

An electron in a crystalline solid experiences the potential from all the other atoms of the solid. The allowed energy levels for that electron are therefore different from the allowed levels in an isolated atom.

There are two general approaches within the framework of the one electron approximation to determining energy levels for electrons in crystals.

The first approach is to consider a system of isolated atoms. An electron in any one of these atoms will have certain allowed energy levels. The energy levels will be determined by solving the appropriate Schroedinger equation. The allowed energy spectrum will consist of a series of discrete energy levels and a continuum corresponding to ionisation of the atom. On bringing together the atoms to form a crystal these discrete energy levels will interact to form bands of allowed energy separated by bands of forbidden energy. The perturbations will be greatest for the outermost electrons. This is the Heitler-London model. It is convenient when the binding of the electrons to the nuclei is strong and there is little perturbation. Thus it is a good approach for dealing with ionic crystals. In the limit, with no interaction, the electrons are confined to discrete

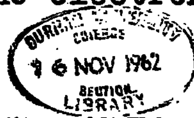

energy levels in the crystal.

The second method is to consider the motion of an electron in the potential of the periodic lattice. The electron is assumed to belong to the whole of the crystal and is not associated with any particular atom. This method is originally due to Bloch. It is more appropriate to use this approach where the binding is weak. Thus it is appropriate for metals where the valence electrons are shared by all the atoms of the crystal.

The second approach has also been applied to crystals with covalent binding and to crystals with mixed ionic-covalent binding. It explains the differences between insulators semiconductors and metals in quantitative terms. The forbidden bands of energy in the Bloch model may be thought of as those energies with which an electron would suffer Bragg reflection, i.e. an electron with a wavelength satisfying the Bragg reflection law for the lattice cannot move freely through the crystal.

In the limit, with no binding, the energy spectrum becomes a continuum corresponding to free electrons.

1.2 Metals, insulators and semiconductors

The Heitler-London model and the Bloch model describe the allowed energies of electrons in crystals. Completely ionic crystals are excluded from this work so that the Bloch method is more appropriate to our discussion. The possible

energy levels of an electron in a crystal form bands of allowed energy which are separated by regions of forbidden energy. Any band of allowed energy is composed of a number of discrete energy levels which are close enough together to be considered to comprise a continuum within that band. It is the number of discrete energy levels within a band, and the number of electrons available to fill these levels, which determine the electrical properties of a crystalline solid.

At the absolute zero of temperature, the allowed energy bands of a given crystal will be filled with electrons up to some maximum energy. The highest filled band contains electrons which are least tightly bound to the nuclei. Thus they will be the valence electrons and this band is termed the valence band. The next highest allowed energy band is termed the conduction band. Energy band diagrams usually refer only to these two bands.

Metals are characterised either by half full valence bands or by overlapping of the conduction and valence bands. When an electric field is applied charge transport can occur as an electron can gain energy from the field.

Insulators and semiconductors are characterised by a completely full valence band and an empty conduction band. At any temperature above absolute zero some carriers will be thermally excited into the conduction band from the valence band. The concentration of carriers in the conduction band

depends on the temperature and the width of the forbidden gap between the top of the valence band and the bottom of the conduction band. The distinction between an insulator and a semiconductor is purely arbitrary. Generally, crystals with a band gap of the order of 1eV or less are termed semiconductors. Crystals with band gaps higher than 2eV are usually considered to be insulators.

1.3 <u>Effective mass of electrons</u>

According to the Bloch model, electrons within an allowed band are free to move anywhere in the solid. However, the relationship between the electron energy and crystal momentum is not the same as that for a free electron moving in a periodic potential. The electron can be considered free by defining an effective mass m^*, which varies with the energy of the electron. For electron energies near the top of any band, m^* is negative, and for electron energies near the bottom of any band, m^* is positive. Electrons with energies near the top of a band may be thought of as carriers with negative charge and mass. It is more convenient to consider conduction at the top of a band as due to positive holes. Thus a hole has a positive charge and a positive mass. The concept of effective mass is invalid at the centre of a band, here the crystal momentum would be infinite. ~~For electrons with energies near the centre of a band, the relationship between the electron energy and crystal momentum is that for an electron moving in~~

~~a periodic potential with no binding.~~

1.4 Concept of mobility

The movement of carriers in a crystal is conceived as a drift superimposed on the random thermal motion of electrons. The drift mobility μ is the drift velocity in unit field. In pure crystals, and at low fields, electrons are scattered by the acoustical vibrations of the lattice, and it can be shown that

$$\mu \propto T^{-3/2} \qquad 1.4 \ (a)$$

Irregularities and impurities in a crystal lattice introduce scattering which alters the temperature dependence of the mobility.

Generally the mobility is assumed independent of the field. This implies that the total energy of the carriers remains unchanged by the field and the electrons are in thermal equilibrium with the lattice.

It is convenient to define two mobilities for charge carriers in a crystal, one for electrons and the other for holes.

1.5 The Fermi level

A function can be defined which determines the probability of an energy state being occupied by an electron at a given temperature. Such a function is the Fermi-Dirac distribution function. The energy level at which the probability of a state being occupied is one half is the Fermi level. The Fermi-Dirac

distribution function is

$$f(E) = \frac{1}{e^{\frac{E - E_f}{kT}} + 1} \qquad 1.5\ (a)$$

where E_F is the Fermi level and E is the energy level for which the probability of occupation is f(E), at an absolute temperature T.

1.6 Density of states and carrier distribution

The concentration of electrons, n(E)dE, with energies lying between E and E + dE must equal the concentration of available levels in this energy range, multiplied by the probability that an electron will occupy each of those levels. Thus

$$n(E)dE = g(E)f(E)dE \qquad 1.6\ (a)$$

in thermal equilibrium. The function g(E) is the density of states per unit volume. It can be shown that in the simple case of spherical energy surfaces in k-space, (1), the density of states in the conduction band is

$$g(E) = \frac{1}{2\pi^2} \left(\frac{2m^*}{\hbar^2} \right)^{3/2} E^{1/2} \qquad 1.6\ (b)$$

where $\hbar = \frac{1}{2\pi}$ x Planck's constant and E is measured from the band edge. For a perfect crystal there are no states in the forbidden gap, except those due to the surface. The surface is an abrupt discontinuity in the lattice and this break in

periodicity introduces states in the forbidden gap of insulators and semiconductors. These states are localised energy levels at the surface.

Equation 1.6 (a) determines the density of carriers per unit volume in the energy range E to E + dE. Integration of this equation gives the total number of carriers in the conduction band.

For an insulator, or intrinsic semiconductor where $\frac{E - E_F}{kT} \gg 1$, we have the simplifications.

$$f(E) = \exp \frac{-(E - E_F)}{kT} \qquad 1.6\ (c)$$

$$E_F = \frac{-E_G}{2} + \frac{3kT}{4} \log \frac{m_h^*}{m_e^*} \qquad 1.6\ (d)$$

where E_G is the width of the forbidden gap, and m_h^* and m_e^* are the effective masses of holes and electrons respectively.

The number of electrons in the conduction band is

$$n = 2\left(\frac{2\pi m_e^* kT}{h^2}\right)^{3/2} \exp -(E_C - E_F)/kT \qquad 1.6\ (e)$$

Equations 1.6 (c) (d) (e) are valid provided $E - E_F \gg kT$, which will be true for insulators. The density of holes in the valence band is given by 1.6 (e) with m_e^* replaced by m_h^* and $E_C - E_F$ replaced by $E_F - E_V$.

From equation 1.6 (c), the probability of occupation decreases exponentially with the energy of the state above

the Fermi level. The hole probability can be expressed as $F_h(E) = 1 - F_e(E)$.

The simplifications, 1.6 (b) (d) (e), all assume the effective mass is independent of the direction through the crystal.

A donor (acceptor)level can be defined as a discrete allowed energy level in the forbidden gap with an electron (hole) associated with the level. Thermal ionisation of the electron (hole) from the level into the conduction (valence) band leads to n-type (p-type) conductivity. The allowed level is localised in the crystal. Other allowed energy levels in the forbidden gap are discussed in 1.11.

The band theory of solids can be explored further in the texts of ref. 1.

1.7 Conduction mechanisms in insulators

The insulators to be considered are those materials for which the band theory is appropriate. Crystals with tight binding and very narrow allowed energy bands are excluded. The energy band scheme for an insulator is illustrated in fig. 1.7.1. The energy gap E_G is large compared to the thermal energy of the electrons at all working temperatures. There can be no net transfer of charge in a completely full band.

Mott and Gurney (2) pointed out that conduction would be possible if electrons could be supplied to the empty conduction band. Hole conduction would also be possible if electrons

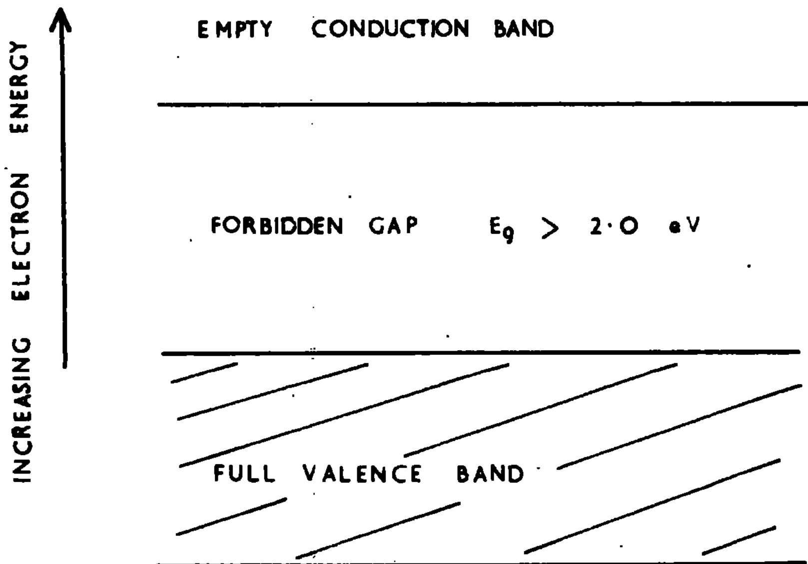

FIG 1.7.1

ENERGY BAND SCHEME FOR AN INSULATOR

could be removed from the valence band. In both instances, the space charge of the current carriers would limit the flow of current.

A close analogy can be drawn between conduction by these mechanisms and thermionic emission and subsequent space charge limited conduction in a vacuum diode. In the solid state the drift velocity of the carriers is limited to $E\mu$, where E is the applied field and μ the mobility of the carriers. This introduces significant differences between the two conduction processes.

1.8 Analysis of Mott and Gurney

The situation analysed by Mott and Gurney was that in which the work function of the metal contact was less than the work function of the insulator. It can be shown (1) that the work function is equivalent to the energy required to remove an electron from the Fermi level of a crystal to a point at rest outside the crystal. The energy level diagram for a contact of this nature is illustrated in fig. 1.8.1. The energy zero is the energy of an electron at rest outside the metal. On making contact electrons would flow into the empty levels of the insulator. In equilibrium, when the Fermi levels are equal, the space charge of the electrons in the insulator would prevent further flow, and the bottom levels of the conduction band would be distorted as illustrated.

The number of electrons, No, per unit volume, just inside

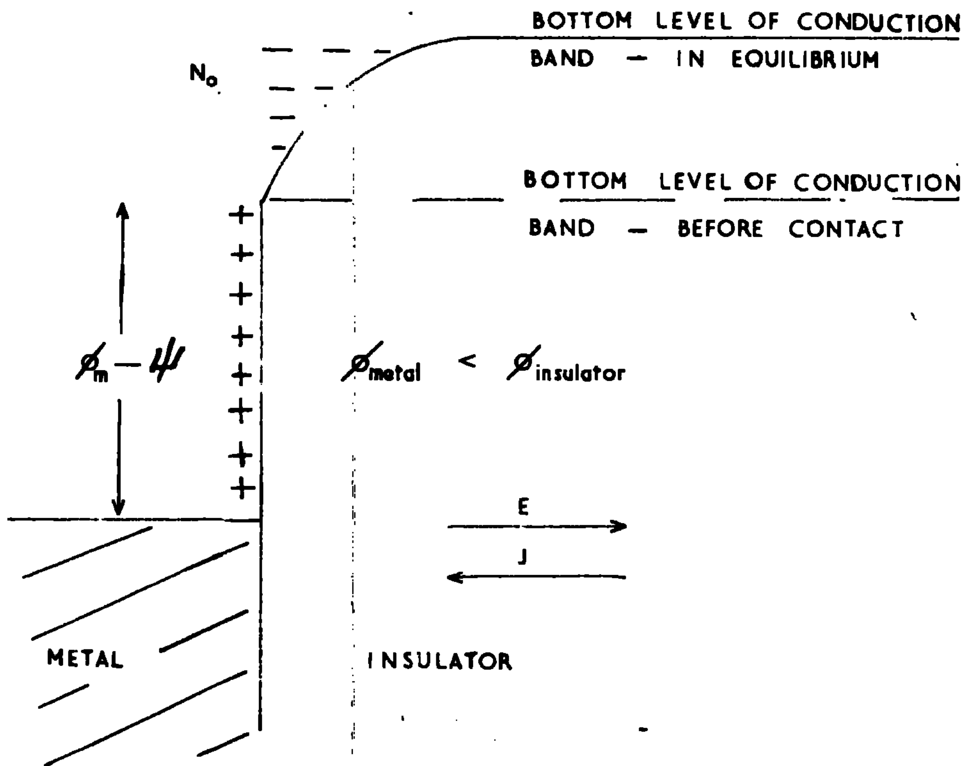

FIG 1.8.1

THE METAL - INSULATOR CONTACT

MOTT AND GURNEY

the insulator is given by

$$No = 2\left(\frac{2\pi m_e^{*} kT}{h^2}\right)^{3/2} \exp\left[-(\phi - \psi)/kT\right] \qquad 1.8\ (a)$$

ϕ Work function of the metal, (eV). m_e^{*} Effective mass of the electron

ψ Electron affinity of the insulator, (eV). h Planck's constant.

This result is derived in ref. 1. It is determined by evaluating 1.6 (a). i.e. the product of the Fermi-Dirac distribution function for a metal and the density of states function of an insulator. [1.5 (a). 1.6 (b)] It embodies the assumption $\phi - \psi \gg kT$.

From equation 1.8 (a), the number of electrons available to an insulator, at room temperature, is

$$No\ /cc \approx 10^{19} \exp \frac{-(\phi - \psi)}{kT} \qquad 1.8\ (b)$$

Thus typical values are

$\phi - \psi$	eV	0.1	0.5	1.0
No	cm^{-3}	10^{17}	10^{10}	10^{2}

Mott and Gurney considered two basic equations.

(i) Poisson's Equation

$$\frac{dE}{dx} = \frac{ne}{\epsilon} \qquad 1.8\ (c)$$

(ii) A current flow equation

$$J = \mu enE - e D\frac{dn}{dx} \qquad 1.8\ (d)$$

This states that the total current is the sum of the diffusion component, $e D \frac{dn}{dx}$, and the drift component μenE. With no applied voltage, the two are equal and opposite and no net current flows.

Their analysis being converted to the rationalised m.k.s. system of units, the directions of J and E are shown in fig. 1.8.1.

E Field intensity
J Current density
d Distance between electrodes
x Distance from cathode
n Number of carriers, cm^{-3}
D Diffusion coefficient
ϵ Permittivity of insulator [Dielectric constant x Permittivity of free space].

Mott and Gurney eliminated n from 1.8 (c) and 1.8 (d) and integrated the resulting equation, this gave

$$J x + \text{constant} = \tfrac{1}{2} \mu \epsilon E^2 - D \frac{dE}{dx} \qquad 1.8 \text{ (e)}$$

For diffusion to be small compared with the drift component

$$\tfrac{1}{2} \mu \epsilon E^2 \gg D \frac{dE}{dx}$$

This condition becomes

$$\frac{E \epsilon}{2} \gg \frac{kT}{ed}$$

on using Einstein's relation $e D = kT\mu$ and the approximation $\frac{dE}{dx} \approx \frac{E}{d}$.

Thus on putting $E = V/d$, the condition for the diffusion

to be small is obtained.

$$V \gg \frac{kT}{e}$$

This condition is satisfied at room temperature for $V \gg$ 25 millivolts.

Under these conditions the diffusion term in 1.8 (e) can be neglected and the equation reduces to

$$J. \quad x. \quad + \text{constant} \quad = \tfrac{1}{2}\mu\epsilon E^2 \qquad 1.8\ (f)$$

Mott and Gurney evaluated the constant by putting n = No at x = 0. Thus on re-arrangement

$$E = \left[\frac{2J}{\epsilon\mu}(x + x_o)\right]^{\frac{1}{2}} \qquad 1.8\ (g)$$

where $$x_o = \frac{\epsilon J}{2\mu No^2 e^2} \qquad 1.8\ (h)$$

Finally on integrating 1.8 (g) they obtained

$$V = \frac{2}{3}\left\{ \left(\frac{2J}{\epsilon\mu}\right)^{\frac{1}{2}} \left[(d + x_o)^{3/2} - x_o^{3/2}\right]\right\} \qquad 1.8\ (i)$$

This gives, using 1.8 (h) and 1.8 (i) the relation between V and J. In particular, for small current, $x_o \ll d$.

$$J = \frac{9}{8}\ \frac{\epsilon\mu V^2}{d^3} \qquad 1.8\ (j)$$

and for large currents, $x_o \gg d$.

$$J = e\mu No\frac{V}{d} \qquad 1.8\ (k)$$

This analysis predicted that space charge limited currents should vary as the square of the applied voltage and the inverse cube of the thickness, equation 1.8 (j). For voltages high enough for space charge effects to be small, the current should obey Ohm's law, equation 1.8 (k). This work of Mott and Gurney is open to criticism on the evaluation of x_o, and the deduction of equation 1.8 (k) for $x_o \gg d$.

The metal-insulator contact under an applied voltage is illustrated in fig. 1.8.2. The energy level of the bottom of the conduction band is distorted, and electrons have to surmount the energy maximum to contribute to the current. According to equation 1.8 (g) the field is zero at $x = -x_o$. Thus the potential minimum in Mott and Gurney's situation would be at $-x_o$. Consequently the evaluation of x_o in this work is equivalent to putting the metal-insulator contact [x = o] at a distance x_o to the right of the potential minimum, fig. 1.8.2.

Decreasing x_o would displace this zero towards the potential minimum, and for $x_o \ll d$, the zero could be taken at x_o with small error. This is the condition for the validity of equation 1.8 (j). The condition $x_o \gg d$, implies the removal of the metal-insulator contact to the right of the anode. This has no physical significance and the deduction of equation 1.8 (k) is invalid.

The position can be clarified by a different evaluation of x_o.

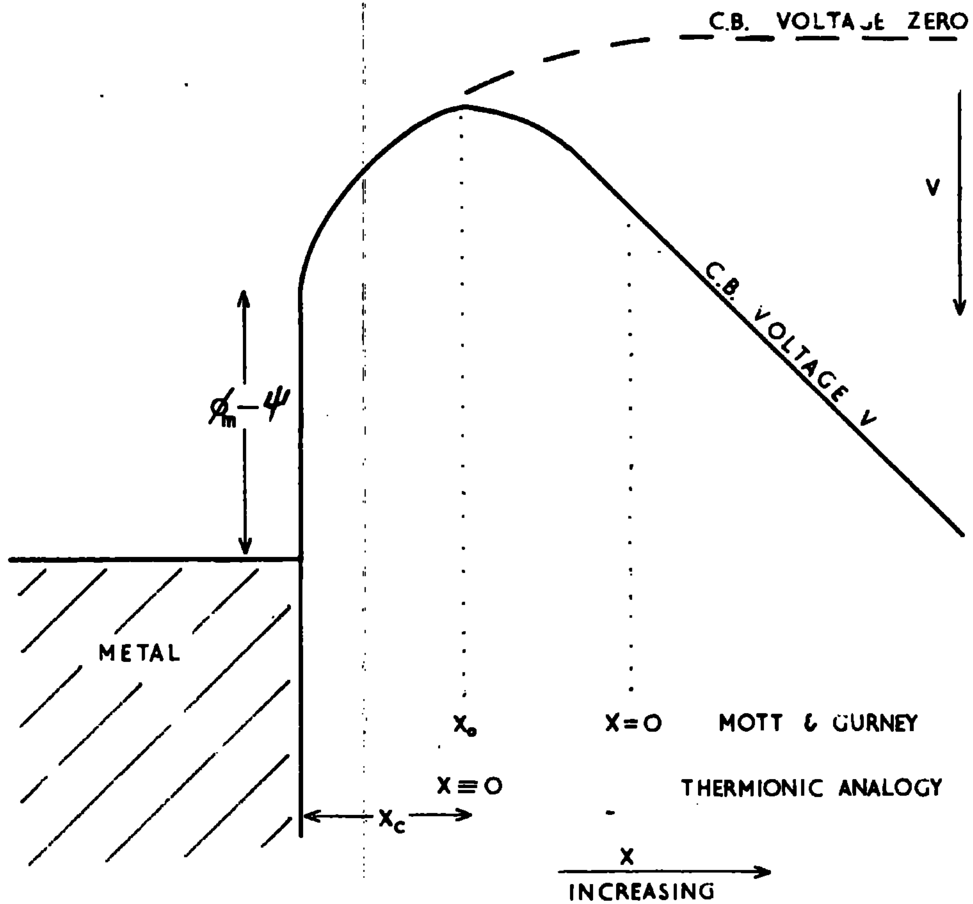

FIG 1.8.2

THE METAL-INSULATOR CONTACT

UNDER AN APPLIED VOLTAGE

1.9 Modified Analysis - Thermionic Analogy

An alternative method of evaluating the constant of equation 1.8 (g) is to assume the condition E = 0 at x = 0. Thus, from 1.8 (g), the constant of integration is zero, and we have

$$J = \frac{9}{8} \epsilon \frac{\mu V^2}{d^3} \qquad \begin{matrix} 1.9\ (a) \\ 1.8\ (j) \end{matrix}$$

This is equivalent to putting the metal-insulator contact at the potential minimum (X_c from the cathode). Negligible error is introduced for $x_c \ll d$. This deliberate choice of zero expresses the final result obtained by Mott and Gurney more precisely.

The choice of zero at the potential minimum is the approximation made in deducing Child's law for the thermionic diode.

$$J = \frac{4\epsilon_o}{9} \left(\frac{2e}{m}\right) \frac{V}{d^2}^{3/2} \qquad 1.9\ (b)$$

In the vacuum diode, emitted electrons are continuously accelerated, whereas in the solid state their velocity is limited to $E\mu$. This accounts for the different forms of 1.9 (a), (b). In the vacuum diode, the space charge can become small as the cathode saturates, and saturation will set in at a current determined by the work function of the cathode. In the solid state, a similar saturation is also expected, but in addition an ohmic region will occur before saturation is reached. The ohmic region will appear at sufficiently high voltages for space charge to be negligible, and where a constant number of

carriers N_0 [equ. 1.8 (b)] can still be maintained at the cathode. ~~This is a contact effect, and only appears because the velocity in the solid is limited to Eμ~~.

Under these conditions the current would be that predicted by Mott and Gurney, equation 1.8 (k), and the transition from a square law to Ohm's law is given by equating 1.8 (k) and 1.8 (j). Thus, at the transition

$$\epsilon V \approx e N_0 d^2 \qquad 1.9\ (c)$$

Equation 1.8 (k) is Ohm's law for an insulator with a constant number of carriers available to the conduction band. Mott and Gurney derived 1.9 (c) but this was based on equation 1.8 (k) which was not rigorously derived. Schockley and Prim,[3] and Wright[4] have considered space charge limited conduction in semiconductors and insulators respectively, with the same approximations used in this section. They come to the same conclusions.

1.10 Contact Limitations

Neglecting high field effects, (Schottky Effect, Field Emission) the saturation current for a thermionic emitter is

$$i = \frac{4\pi m e k^2}{h^3} T^2 e^{\phi/kT}$$

This is derived in ref. 1 (b) p.55 ff. This gives an upper limit to the current that can be drawn through an insulator from a metal contact. For an insulator with an

electron affinity ψ

$$i_s = \frac{4\pi m^* e k^2}{h^3} T^2 \; e^{-\frac{(\phi - \psi)}{kT}} \qquad 1.10\ (a)$$

Thus, typical values at room temperature are:

$\phi - \psi$ eV	0.1	0.5	1.0
i_s amps/cm^2	$4.0\ 10^{4}$	$4.0\ 10^{-3}$	$4.0\ 10^{-11}$

The field for saturation is given by equating i_s (1.10 (a)) and Ohm's law, equation 1.8 (k)

$$\frac{4\pi m^* e k^2}{h^3} T^2 \; e^{-(\phi - \psi)/kT} = e\mu\, No\, E$$

Substituting the value for No, equation 1.8(a)

$$\mu E = \left(\frac{kT}{2\pi m^*} \right)^{1/2} \qquad 1.10\ (b)$$

Thus for $\mu \approx 250$ cm^2/volt. sec., saturation occurs at a field of 10^4 volts/cm, the 'ohmic' saturation field.

This result is valid when all the available carriers are moved through the crystal, thus it only holds when space charge effects are small. Physically the limit is reached when the ~~velocity~~ rate of passage of the carriers through the insulator equals the mean ~~velocity~~ rate with which carriers can be supplied by the contact. This will be valid under the assumption of no high field effects.

When space charge limits the number that can be removed per second, saturation will occur at a higher field. This may be estimated by equating 1.9 (a) to the saturation current, i_s

$$i_s = \frac{9}{8} \mu \epsilon \frac{E^2}{d} \qquad 1.10\ (c)$$

Thus, when space charge is limiting the current flow, saturation occurs at a field

$$E_s = \left(\frac{8}{9} \quad \frac{d \ i_s}{\mu \epsilon} \right)^{1/2} \qquad 1.10\ (d)$$

For an insulator 10^{-3} cms thick, with permittivity = 10, and μ = 250 cm^2/volt. sec, values of i_s and E_s would be

$\phi - \psi$ (eV)	0.1	0.5	1.0
i_s amps cm^{-2}	4.0 10^4	4.0 10^{-3}	4.0 10^{-11}
E_s volts. cm^{-1}	1.2 10^6	3.6 10^2*	3.6 10^{-2}*
S.C.L. - Ohm's law transition (Volts.cm^{-1})	-	2.0 10^1	2.0 10^{-7}

For the two values *, the saturation field is below that for ohmic conduction and 1.10 (d) is not valid. The saturation is then at 10^4 volts/cm, space charge having become small. The transition from a square law to Ohm's law is given by 1.9 (c). It is

$$\epsilon E = edNo \qquad 1.10\ (e)$$

Inserting the values of No, this gives the transition

voltages shown.

The condition for an ohmic region on the characteristic is found by inserting the 'ohmic' saturation field in 1.10 (e). It is

$$No \leqslant 5.0 \; 10^9 \text{ electrons/cc.}$$

Thus there will be an ohmic region if $\phi - \psi > 0.5eV$, for an insulator with the assumed parameters.

1.11 <u>Levels in the Forbidden Gap</u>

In any practical insulator there are a number of allowed electronic energy levels in the forbidden gap. These can be associated with impurities in the insulator or with defects in its structure. Vacancies, interstitial atoms and dislocations are among the structural defects that can give rise to levels in the forbidden gap. The allowed energy levels are localised at the imperfection.

It is convenient to discuss the effects of these localised levels or centres in terms of two mechanisms. (1) Trapping (2) Recombination.

(1) Trapping refers equally well to electrons and holes, but for clarity only electron traps are discussed. Three distinctions are made (a) Levels within kT of the conduction band (b) Levels between the conduction band ~~the~~ and the Fermi level (c) Levels below the Fermi level. The Fermi level is that energy level at which the probability of finding a level occupied is one half (1.5). Assume electrons are injected into

the conduction band and the shift in the Fermi level is negligible. Consider the effects of these trapping levels. Levels (a) would be in thermal equilibrium with the injected electrons and would have negligible effect on the current flow. These levels are termed 'shallow' traps. Levels (b) would trap a fraction of the injected charge. At any given time there would be a fraction of the injected charge in such traps. This would reduce the current flow by the ratio of the number of free carriers to the total number injected. Levels (c) would always be full and would have a fixed space charge associated with them. ~~It is reasonable to assume that this would introduce a voltage threshold below which it would not be possible to inject carriers in large numbers into the conduction band. This is the basis of Lampert's theory (5) of space charge limited currents in an insulator with traps.~~ Levels (b) and (c) which are far removed from the conduction band (compared with kT) are termed 'deep' traps.

(2) Recombination of electrons and holes is a concept of particular importance in photoconductivity, and in two carrier space charge limited conduction. The capture cross-section of a centre can be defined by

$$\tau = (v\, SN)^{-1} \qquad 1.11$$

τ Free lifetime of carrier

S Capture cross section for carrier

N No. of centres per unit volume

v Thermal velocity of the carrier.

In practice τ varies from 10^{-10} to 10^{-2} secs, and S from 10^{-12} to 10^{-22} cm^2. For an uncharged centre $S \approx 10^{-15}$ cm^2 would be expected.

A centre has two capture cross sections, one for a free electron and one for a free hole, depending on which state it is in. A level may capture an electron and then capture a hole or vice versa, thus aiding direct recombination. The energy may or may not be given out as photons. The two cross-sections determine the behaviour of a level as a recombination centre.

A level may act as a recombination centre or as a trapping level. The distinction is made by comparing the probability of thermal ejection of a trapped carrier with the probability of the centre capturing the complementary carrier. At different temperatures levels may act in different ways. Generally levels near the band edges will be traps and levels near the centre of the forbidden gap will be recombination centres.

The production of levels, and their nature, in CdS, is summarised in Chapter Two. A more complete discussion of levels in the forbidden gap of insulators can be found in Bube's book on Photoconductivity (6).

1.12 Summary

To observe space charge limited currents it is necessary to have a thin slab of good insulating material. The contacts must be capable of providing excess carriers and there should be a minimum number of levels in the forbidden gap. If these conditions can be satisfied the current should vary with the

square of the applied voltage.

Chapter II Previous Experimental Evidence

2.1 Properties of Cadmium Sulphide

A great deal of work has been done on CdS, the interest being centred on the material's photoconductive properties. This section deals with properties of pure CdS which are relevant to space charge limited conduction. A review has recently been made by Lambe and Klick (7) and many references are available in Bube's recent book (6).

Cadmium Sulphide can be prepared by a vapour phase technique, either by combining the elements or by sublimation of the compound (8,9,10). It crystallizes with the hexagonal wurtzite structure (11). The crystals are either irregular rods or thin plates. The plates are suitable for the investigation of space charge limited current flow.

When crystals are prepared with no impurities their resistivity is always n-type, and of the order of 10^{12} ohm.cm. Absence of p-type conductivity is ascribed to high activation energies for p-type impurities (12,13). Several levels in the forbidden gap have been identified (14,15,16) and they may be summarized.

Impurity	Group	Substitutes for	Donor or Acceptor	eV below Conduction band	eV above Valence band
Cl.Br.I	VII	Sulphur	D	0.03	
Al Ga.In	III	Cadmium	D	0.03	
Cu.Ag	I	Cadmium	A		1.0
Cd.vacancy			A		1.0

Measurements of optical absorption have been made at different temperatures (17.18), and the photoelectromagnetic (PEM) effect (19) has been measured at room temperature. The width of the forbidden gap depends on the criteria chosen to define it. A commonly accepted value for CdS at room temperature is 2.4eV.

Kroger et al (20) have measured the Hall effect, resistivity and thermoelectric power of pure CdS, from 20° to 200°K. They conclude that the room temperature mobility of electrons is 210 $cm^2 volt^{-1} sec^{-1}$, and the effective mass is of the order of 0.2 of the electronic mass. From investigations of 'primary' photocurrents, van Heerden (21) puts a lower limit of 0.3 - 3.0 $cm^2 volt^{-1} sec^{-1}$ on the mobility of holes in CdS.

Measurements on evaporated layers by Shuba (22), using a photo-electric technique, put the work function of CdS of the order of 5.7eV. Preliminary investigations by Scheer and Laar (23), using a similar technique, indicate the work function, for a freshly cleaved surface of a single crystal, is of the order of 7.0eV. Smith (24) quotes a value of 4.2eV for a single crystal. This latter value was obtained by measuring the landing potential of a low velocity scanning beam, the work function being measured relative to two dots of gallium and silver on the surface of the crystal.

Edge emission is another important property of pure cadmium sulphide (25). When cadmium sulphide at 77°K or below is irradiated with light of wavelength equal to, or shorter

than, that of the absorption edge, luminescent emission is observed. This emission consists of a series of equally spaced narrow bands between 5100Å and 5600Å. It has been pointed out (25,26) that the energy difference between peaks corresponds closely to the energy of normal lattice vibrations. It is reasonable, therefore, to attribute the peaks to phonon-photon transitions. The emission is due to recombination of electrons and holes. Work by Lambe, Klick and Dexter (27) suggests this recombination takes place via a centre, i.e. a trapped electron recombining with a free hole. After exciting a crystal and producing edge emission they placed the crystal in the dark. On irradiating with infra-red, edge emission was stimulated. They postulated that the infra-red produced free holes which then combined with trapped electrons. In view of this evidence it seems unlikely that excitons are involved in this recombination There is evidence for excitons in the absorption and emission spectrum of CdS in the range 4800Å - 5050Å, it is reviewed in ref. (7), but this can be distinguished from the edge emission.

Discussion of speed of response and maximum gain of cadmium sulphide is ~~defined~~ deferred until Chapter III, as are general photoconductive properties.

2.2 The Metal-Insulator Contact

Work by Smith (24) showed that indium or gallium could make ohmic contact to cadmium sulphide. An ohmic contact is one that is capable of injecting excess carriers over and above those

required to support Ohm's law currents for the bulk material. Smith found that pressed contacts were satisfactory, no chemical reaction took place at the contacts, and diffusion of the indium or gallium into the crystal was not necessary. He found a rectifying contact could be made to the crystal by applying either a gold or silver electrode. The forward current was of the order of 1mA and the reverse current less than 10^{-9} amps, with up to 10 volts applied across 10^{-2} cms of crystal.

Smith suggested that an ohmic contact should be characterized by

(i) Maximum performance of the crystal as a photoconductor.

(ii) Linear current-voltage characteristic at low voltages. In his work this corresponded to fields of the order of 10^3 volts/cm.

(iii) Absence of photo-voltaic effects.

(iv) Photo-current noise associated only with the noise of the photon stream.

(v) Current limited only by space charge effects and not by the supply of carriers at the electrodes.

In the linear regime (ii), there is no significant injection and the current is carried by the small number of carriers already present in the conduction band.

It was suggested that indium (or gallium) formed ohmic contacts on CdS because the work functions of the metals are less than that of cadmium sulphide. With a low work function contact there would be a ready supply of carriers to the con-

duction band as $(\phi - \psi)$ would be small (1.8). With a high work function contact such as gold or silver, a Schottky exhaustion barrier would be set up and the number of carriers available to the conduction band would be sharply reduced. The scanning technique (2.1) quoted by Smith determined the work functions of silver, gallium and CdS as 4.9eV, 3.6eV and 4.2eV respectively.

Energy level diagrams for the ohmic and rectifying contact are illustrated in figs. 2.2.1 and 2.2.2 respectively.

Surface effects would introduce localised levels in the forbidden gap. Smith suggested that the low work functions of indium and gallium could counteract the effects of these surface states. (1.6).

Work by Buttler and Muscheid (28,29) revealed that any metal can make ohmic contact to CdS, provided the surface has been previously exposed to electron or ion bombardment. Fassbender (30) reported that ohmic contacts could be produced if the contact area was subject to ionic bombardment before application of the contact., He deduced that a low resistivity surface layer was created on the crystal due to the formation of sulphur vacancies. These would act as donors (12). Alfrey and Cooke (31) found indium contacts to ZnS were ohmic if either, (i) the contact was heated to 600°C, or (ii) a high current was passed to 'form' the contact. Further, after this 'forming', any metal would make ohmic contact on this 'formed'

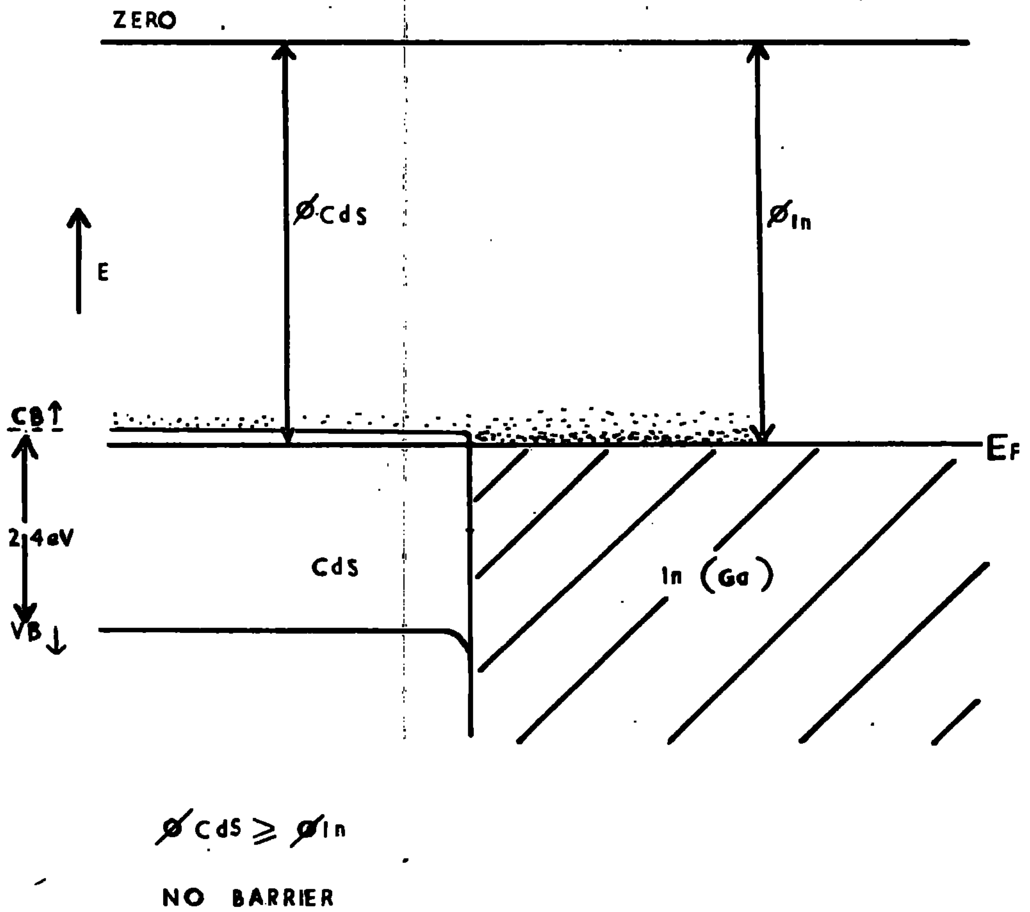

FIG. 2.2.1

OHMIC CONTACT

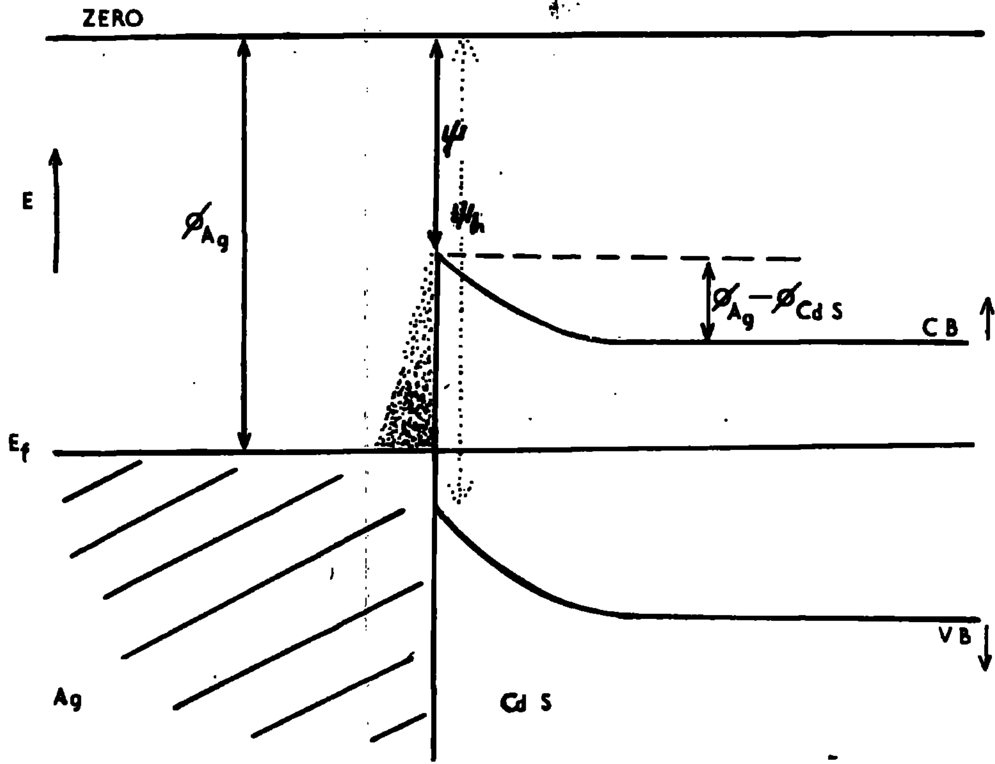

$\phi_{CdS} < \phi_{Ag}$

ψ ELECTRON AFFINITY OF Cd S
ψ_h HOLE " " "

BARRIER $\phi_{Ag} - \psi$ FOR ELECTRONS
$\psi_h - \phi_{Ag}$ FOR HOLES

FIG 2.2.2.

RECTIFYING CONTACT

part of the crystal.

Kroger et al (32) proposed the model illustrated in fig. 2.2.3. They suggested that diffusion of indium or gallium into the crystal produces a low resistivity layer which acts as the reservoir of carriers for the bulk material. The exhaustion barrier is so thin that electrons can easily tunnel through it. Bombardment of the crystal surface produces a highly conducting layer through which a high work function material can make ohmic contact to the bulk of the crystal.

2.3 Hole injection

There is little evidence for hole injection in CdS (33). By arguments, similar to those of section 1.8, the type of contact needed for hole injection can be determined. Consider the contact illustrated in fig. 2.2.2. Measure the hole energy positive downwards from the zero (1). The barrier presented for hole flow in the valence band is $E_G + \psi - \phi$metal. The hole affinity is related to the electron affinity by $\psi_h - \psi = E_G$. Thus the barrier is $\psi_h - \phi_M$. The density of holes available to the valence band is

$$N_h = 2\left(\frac{2\pi m^* kT}{h^2}\right)^{3/2} \exp\left[\frac{-(\psi_h - \phi_M)}{kT}\right] \qquad 2.3\ (a)$$

This is obtained by a similar analysis to that outlined in 1.6 and 1.8.

From 2.3 (a), the higher the work function of the metal, the more holes there are available to the valence band. Thus

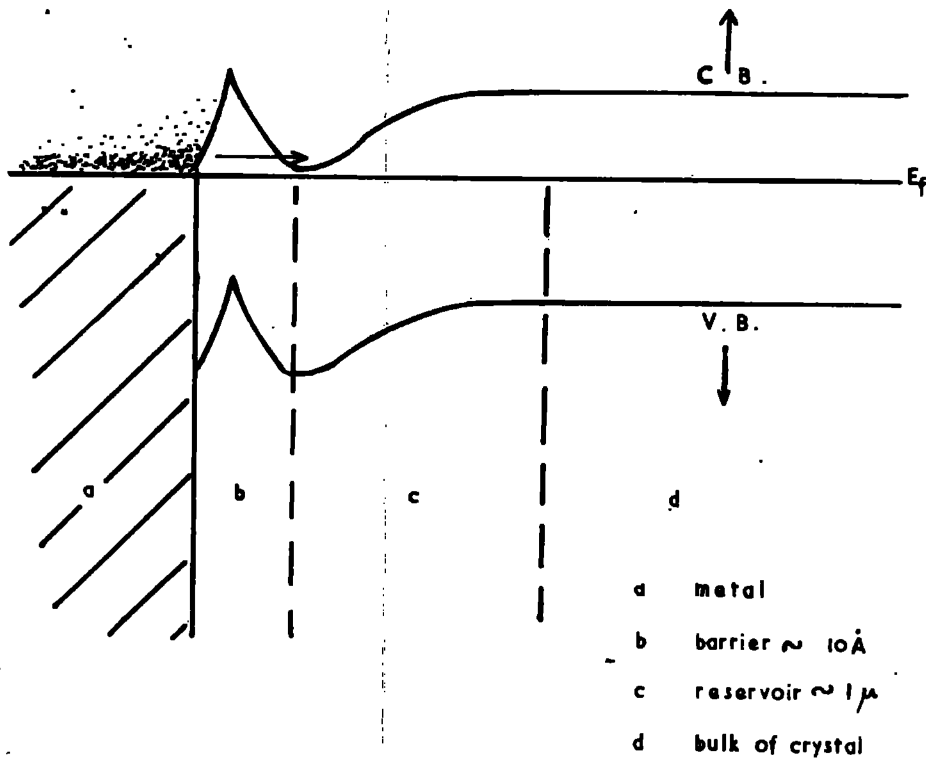

FIG 2.2.3

OHMIC CONTACT

CONDUCTING SURFACE LAYER

for an ohmic hole injecting contact a high work function metal would be required. It might be expected from this type of analysis that it should be possible to correlate the degree of rectification produced with the work function of the non-ohmic contact. In practice, surface states make this type of measurement difficult.

In contrast with the above considerations the contact shown in fig. 2.2.3 is identical to the n^{+}- n junction of normal semiconductor work. When the junction is biased with the n^{+} side positive there is very little hole flow. Thus, this type of contact is ideally suited for study of single carrier electron currents. With a diffused contact, or a contact produced with bombardment, it is not possible to estimate saturation limits in terms of the work function differences.

2.4 Experimental Evidence for Space Charge Limited Conduction

Space charge limited conduction has been investigated in CdS and zinc sulphide by Ruppel (34) and in cadmium sulphide by Wright (4, 35). Dacey (36) has investigated space charge limited (S.C.L.) hole flow in germanium.

This section is concerned with the early work of Smith and Rose (24,37). They found that the current voltage characteristic of a thin plate of CdS with indium electrodes was of the form illustrated in fig. 2.4.1.

Curve 'a' was taken when the current had settled to a reliably stationary value. They found that, initially, on applying a voltage, a high current was observed. This current

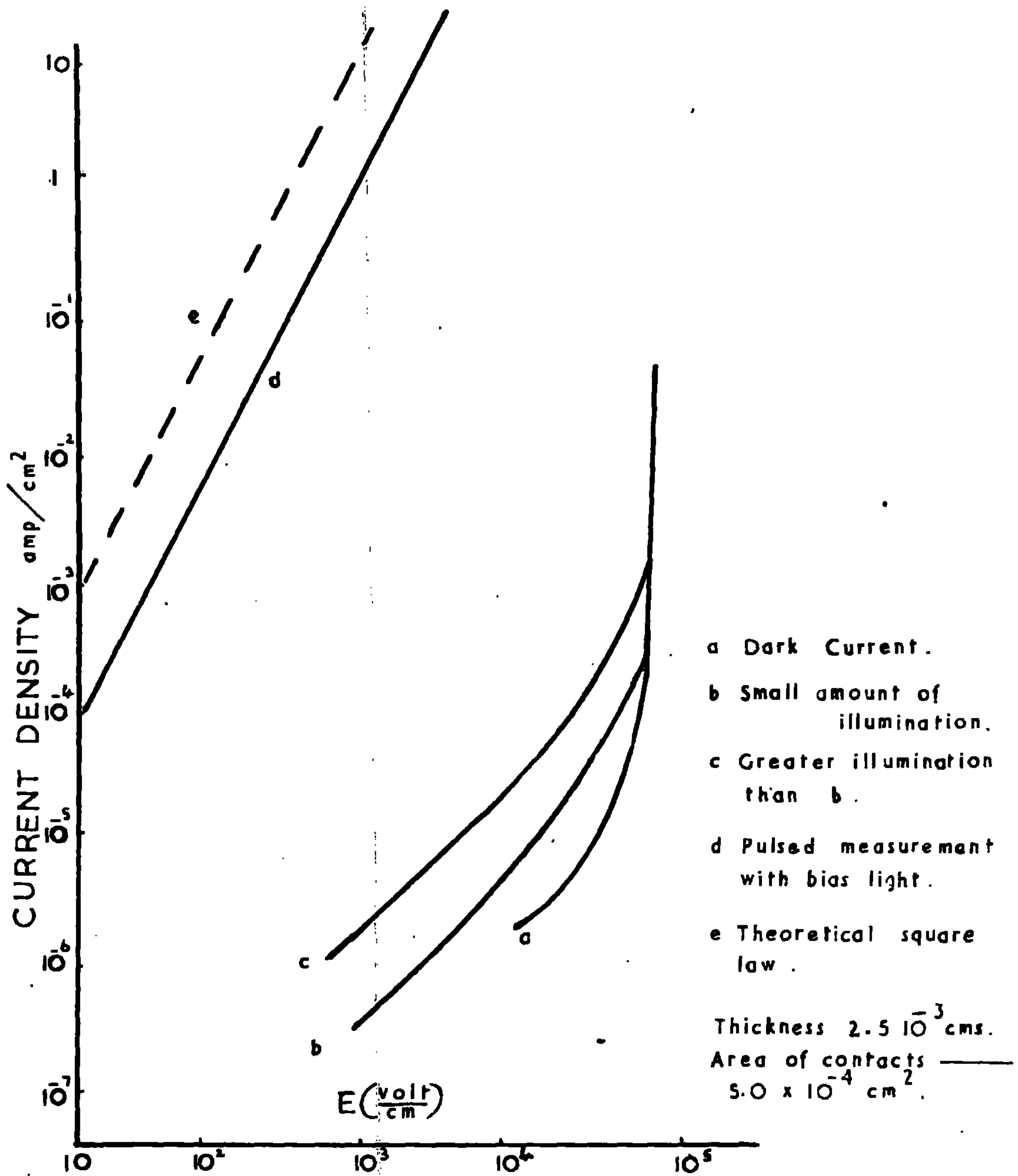

FIG. 2.4.1

CURRENT—VOLTAGE CHARACTERISTICS

—— SMITH AND ROSE.

decreased over a period of hours to a low steady value. The behaviour was explained in terms of electron trapping by the following argument. For a given voltage, a fixed amount of charge is forced into the crystal, the majority of which is trapped. The trapped charge raises the Fermi level and therefore the equilibrium density of carriers in the conduction band. Smith and Rose suggested a good approximation could be made by assuming all the charge is trapped, leading to a re-location of the Fermi level. They then assumed that the allocation of some of the trapped charge to the conduction band to maintain statistical equilibrium would have a negligible effect on the new Fermi level. If a uniform energy distribution of traps in the forbidden gap is assumed, equal increments of voltage will make equal energy shifts in the position of the Fermi level. The free electron density varies exponentially with the position of the Fermi level and therefore the current will vary exponentially with voltage. Any form of current-voltage characteristic can be explained in this manner by assuming an appropriate variation of trap density with energy, in the forbidden gap. Rose et al have discussed the possibility of determining the trap distribution from the current voltage characteristic. (38,39).

When the crystal was illuminated, Smith and Rose obtained curves similar to 'b' and 'c' fig. 2.4.1. An ohmic region of the characteristic is obtained when the volume generated

carrier density predominates over the injected carrier density. This shows that the photocurrent can vary linearly with voltage while the dark current is following some high power law. This makes it difficult to ascribe the latter behaviour to any form of collision ionisation process.

Curve 'd' fig. 2.4.1 was obtained using pulsed voltages with a small bias light on the crystal. It was found that the pulsed dark-currents were higher than the steady direct currents by several orders of magnitude but fell short of the theoretical square law, (curve 'e' equation 1.9 (a)), and did not show a square law dependence of current on voltage. However they found that with a steady bias light on the crystal, reasonable agreement with equation 1.9 (a) was obtained.

Smith and Rose also examined the effects of applying alternating voltages to their crystals. The results yielded essentially the same information. The transient decay was attributed to the time taken for injected charge to condense into traps. From 1.11 the lifetime is proportional to the number of traps, the current therefore would be expected to decrease exponentially with time. Equation 1.11 is a general expression for the lifetime of a free carrier. (6). If more charge is injected into the crystal the traps will fill quicker, thus the decay to a stable current is faster at higher voltages.

Direct observation of stored charge was made by, applying a voltage to the crystal and then, dropping the crystal on to

an electrometer pan. They found that all crystals were negatively charged, which they claimed was due to electrons remaining in deep traps.

In contrast to Smith's interpretation, Boer and Kummel, (40,41) who also found a high power dependence of current on voltage in doped cadmium sulphide crystals, attributed this to either collision ionisation or field ionisation of electrons from traps.

2.5 Evidence for two carrier S.C.L. conduction in Cadmium Sulphide.

Luminescence has been observed in CdS which can be attribute to the injection of holes at the anode. Smith (33), using insulating crystals supplied with gallium contacts, found that it was first necessary to apply a high field to "form" the anode. Once this had been done he found green luminescence, starting at the anode in spots, which spread throughout the crystal as the field was increased. It was necessary to cool the crystal to liquid air temperatures to observe the luminescence. The wavelength of maximum intensity of the luminescence corresponded to the band gap of CdS, and the luminescence had two peaks. Smith concluded that the luminescence was due to recombination of electrons and holes by a mechanism similar to that involved in the production of "edge emission" (section 2.1).

In Smith's experiments the contacts were placed on the same side of a plate of CdS. A more satisfactory method would be

to have them on opposite faces to reduce surface leakage and to reduce the spacing between the electrodes. He found a steep rise in current with voltage, andthat the luminescence occurred at the high current end of the current-voltage characteristic. (At currents of the order of 1 micro A.). The intensity of the luminescence was proportional to the current, and fields of the order of 10^3 volts/cm were sufficient to produce luminescence.

Boer et al (42) and Diemer (43) have observed luminescence in doped CdS. This was attributed to high field effects. Fields of 10^5 volts/cm were employed. Considering the comparatively low fields used in Smith's work, the different deductions could fit their relevant experimental arrangements.

2.6 Object of the Research

Traps can profoundly modify S.C.L. currents in CdS, and Lampert (5) put forward his theory of "One carrier S.C.L. currents in an insulator with traps" to explain the results of Smith and Rose (37). In this theory, which will be discussed more fully in Chapter III, the threshold for S.C.L. conduction is related to the density of traps.

Unpublished work at G.E.C. by Woods showed:

(i) The trap densities for many crystals calculated on the basis of Lampert's theory were abnormally low ($< 10^{12}$ traps per cm^3). This has been verified by Wright (44) and Ruppel (34b) in published data.

(ii) The current/voltage characteristic often displayed a

region of negative resistance.

(iii) The crystals showed abnormally high sensitivity to low-level illumination, [$<$ 1 ft. cdle.], with an abnormally fast response time [$<$ 1 sec.]. This indicated some new mechanism in the photoconductive process. (The Gain-Bandwidth product is discussed in the following chapter).

(iv) Recombination radiation was observed at the S.C.L. current threshold.

It is the object of this work to clarify the position with respect to these effects. They cannot be explained in terms of Lampert's theory.

2.7 <u>Recent work by Ruppel</u>

Ruppel (45) has found that the charge stored in a crystal after passing a current is not always negative, as found by Smith and Rose (37),(section 2.5). He found that at low voltages the charge was negative, but at higher voltages the charge became positive. The variation of stored charge with voltage is shown in fig. 2. 7 .1. The dashed line represents the expected charge, (voltage multiplied by the interelectrode capacitance). This was followed at low voltages. The interpretation of the swing away from this line is that the cathode becomes saturated. Absence of saturation in the dark current is attributed to the onset of collision ionisation of trapped carriers. Ruppel found a critical current density for saturation of the order of 10^{-6} amps/cm^2.

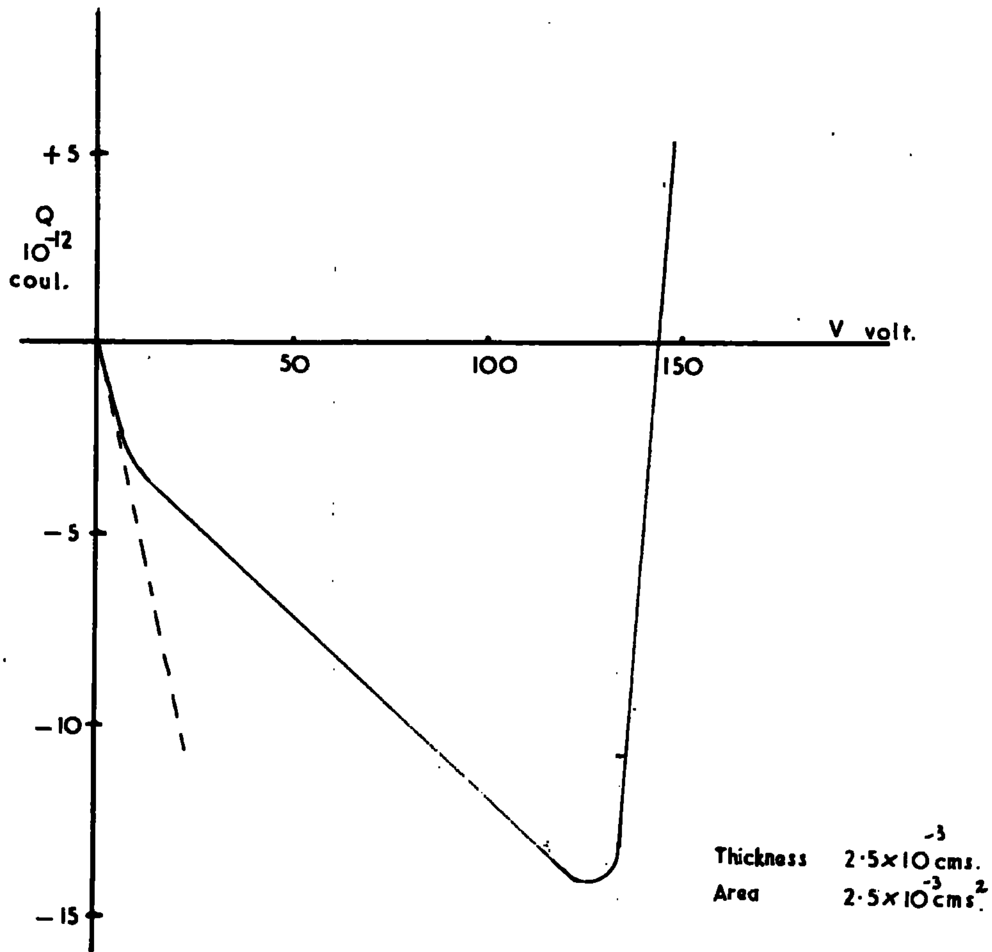

FIG 2.7.1

STORED CHARGE IN CADMIUM SULPHIDE — RUPPEL

Measurements of the photocurrent showed that the current saturated when the charge stored in the crystal became positive. The photocurrent then increased steeply as the voltage was increased, which Ruppel claimed was further evidence for collision ionisation.

From the saturation of the photocurrent, Ruppel calculated the height of the barrier at the cathode to be 0.8eV. He was using pressed indium contacts. With different contacts it is reasonable to expect saturation to occur at higher current densities. In the work of Smith and Rose for example (37), there was no detectable saturation for current densities of the order of 20 amps/cm^2 under pulsed conditions.

2.8 Recent work by Bube

Bube (46) has measured S.C.L. currents at different temperatures. He concludes that the steep rise in current cannot always be interpreted as trap filling effects. He suggests collision ionisation or injection of holes may be responsible in some instances.

Chapter III Theoretical Work

3.1 Basis of Lampert's Theory

A simplified theory of space charge limited conduction in an insulator with traps has been proposed by Lampert (5). He considered conduction by electrons only and assumed a single discrete level of electron traps in the forbidden gap. This is one carrier S.C.L. conduction.

The three basic equations of Lampert's theory are:

$$J = e \mu n E - e D \frac{dn}{dx} = \text{constant} \qquad 3.1\ (a)$$

$$\frac{\epsilon}{e} \frac{dE}{dx} = (n - \bar{n}) + (n_t - \bar{n}_t) \qquad 3.1\ (b)$$

$$n_t(x) = n(x)\ Nt\ [n(x) + N]^{-1} \qquad 3.1\ (c)$$

J current density

ϵ permittivity of insulator

E electric field intensity

e electronic charge

$\bar{n}$ density of free electrons for zero field. (Thermal and Electrical Equilibrium)

$\bar{n}_t$ density of trapped electrons for zero field (Thermal and Electrical Equilibrium).

All functions of position x:

- n density of free electrons
- n_t density of trapped electrons
- E_t energy of trapping level
- E_c energy of bottom of conduction band

N_t trap density

N_c effective density of states in the conduction band

$N = N_c \exp [Et(x) - E_c(x)/kT]$ - compare equation 1.6 (e)

Equation 3.1 (a) is a current flow equation; in Lampert's theory the diffusion term is neglected.

Equation 3.1 (b) is Poisson's equation.

Equation 3.1 (c) is a statistical equation. It assumes that the steady state Fermi level F(x), defined with reference to n(x), determines the occupancy of the electron traps via a Fermi-Dirac occupation function (1.6 (a)).

To solve equations 3.1 (a),(b),(c) Lampert specified two boundary conditions.

$$n(x) \rightarrow \bar{n} \quad \text{as} \quad x \rightarrow \infty$$

$$E = 0 \quad \text{at} \quad x = 0$$

In addition equation 3.1 (a) was replaced by

$$J = e\, n\, \mu\, E = \text{constant} \qquad 3.1\ (d)$$

on neglecting the diffusion term.

Equations 3.1 (b),(c),(d), and the two boundary conditions provided a mathematical basis. Lampert calculated exact solutions from these equations.

The results cannot hold near the cathode for at $x = 0$ $E = 0$. $n = \infty$; and they will not hold when diffusion currents are not negligible. In the absence of an exact theory it is not possible to give a quantitative estimate of the range of validity.

3.2 The Limiting Characteristics

Before presenting the results obtained by Lampert it is convenient to consider the limiting characteristics.

Lampert pointed out that S.C.L. currents will be confined to a triangle. This is illustrated in fig. 3.2.1. which is a log-log plot of current versus voltage.

Curve 'a' of fig. 3.2.1. is Ohm's law for the neutral crystal,

$$J = e \bar{n} \mu E = e \bar{n} \mu \frac{V}{d} \qquad 3.2\ (a)$$

where d is the cathode-anode spacing. The true curve cannot lie below the Ohm's law line, for carriers can only be added, by injection, to those thermally present.

Curve 'b' of fig. 3.2.1. is Childs law for an insulator

$$J_c = \frac{9 \epsilon \mu V^2}{8 d^3} \qquad 3.2\ (b)$$

this represents the situation where all the injected carriers are in the conduction band. The true curve cannot lie above this line.

Curve 'c' of fig. 3.2.1. is the traps-filled-limit curve. This represents the situation where all the traps are filled, and the largest possible fraction of the injected carriers are trapped. The steepness of the traps-filled-limit (TFL) curve follows from the assumption that the trap density Nt is very much greater than the dark density of carriers. A mathematical treatment of the traps-filled-limit law is given by Lampert.

The voltage V_1, fig. 3.2.1. marks the transition from ohmic to space charge limited conduction. The Ohm's law and

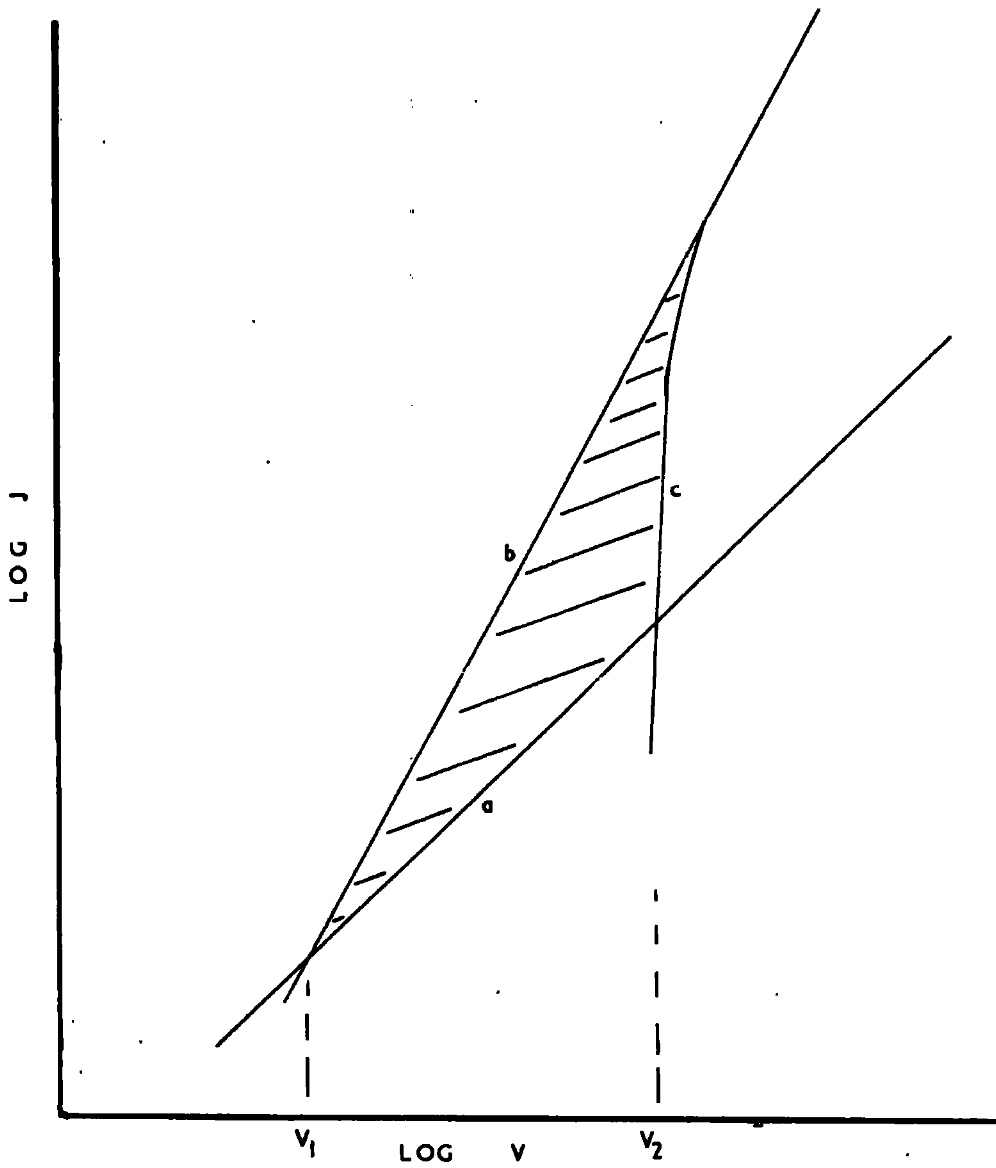

FIG 3.2.1

LIMITING CURRENT - VOLTAGE CHARACTERISTICS

AFTER LAMPERT

Child's law lines meet at a voltage

$$V = \frac{8ed^2 \bar{n}}{9\epsilon} \quad \text{from equating 3.2 (a) and (b)}$$

This transition occurs when the excess injected carrier density exceeds the dark density.

Lampert calculated that the true transition in a trap free crystal will be given approximately by

$$V_1 = \frac{ed^2 \bar{n}}{2\epsilon} \qquad 3.2\ (c)$$

The voltage V_2 is the voltage required to overcome the repulsion of unneutralised charge in traps. Lampert shows that this voltage is given approximately by

$$V_2 = \frac{ed^2}{2\epsilon} Nt \qquad 3.2\ (d)$$

Finally from 3.2 (c) and (d) the ratio of V_2 to V_1 is approximately

$$\frac{V_2}{V_1} \approx \frac{Nt}{\bar{n}} \qquad 3.2\ (e)$$

Thus, with $\bar{n} \approx 10^6$ cm^{-3} and $Nt \approx 10^{14}$ cm^{-3}, non-linearities will be expected over a considerable range of the characteristic of an insulator.

3.3 Results of Lampert's Analysis

From his analysis Lampert concluded that, if the Fermi level at the anode lies below the trap depth, there is a fixed

ratio θ, independent of applied voltage such that

$$\frac{n(d)}{n_t(d)} = \theta = \frac{N_c}{Nt} \exp \frac{E_t - E_c}{kT} \qquad 3.3\ (a)$$

Thus of the total charge density at the anode only the fraction θ is available for conduction. The effectiveness of injected carriers is reduced by the factor θ, and the Ohm's law - Child's law transition (3.2 (c)) is now given by

$$V = \frac{ed^2 \bar{n}}{2\epsilon\theta} \qquad 3.3\ (b)$$

For voltages above this transition but below the T.F.L. curve, the characteristic follows Child's law modified by the correction factor θ.

$$J = \frac{9\, \theta \epsilon \mu}{8d^3} V^2 \qquad 3.3\ (c)$$

Finally at the threshold voltage V_2, the traps fill and the curve follows the T.F.L. line and finally Child's law.

The exact solutions obtained by Lampert are illustrated in fig. 3.3.1.

The reason for considering the charge density at the anode arises from the mathematics on making the assumption that the electric field intensity at the anode is not very different from the 'ohmic' electric field intensity. With this assumption, the situation is identical to that referred to earlier (1.11). Electrons are trapped for some finite

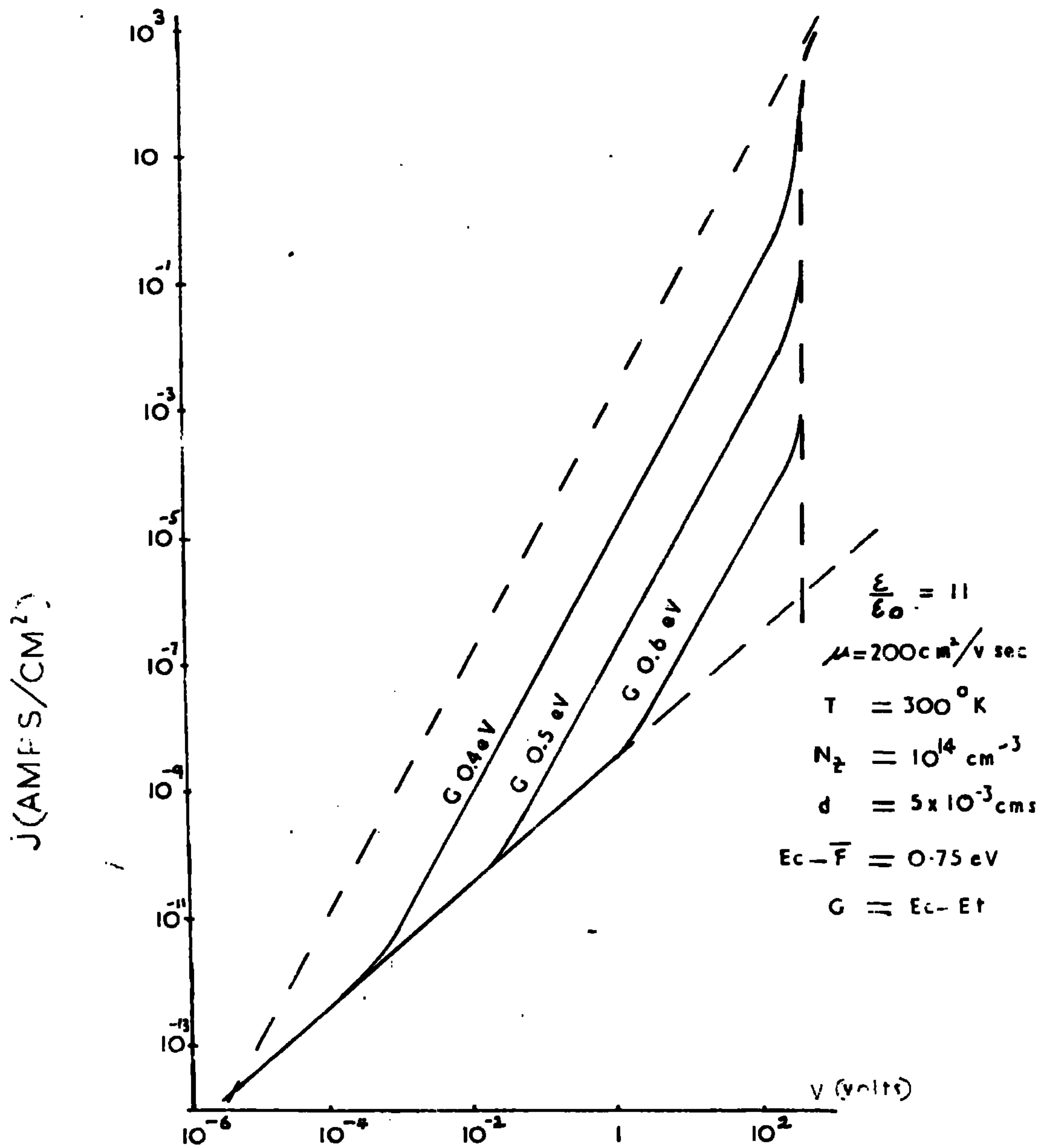

FIG 3.3.1

CURRENT–VOLTAGE CHARACTERISTICS

— LAMPERT

time which leads to a decrease in their drift mobility. For $E_t - F_d > kT$ the time spent by an electron in a trap is independent of applied voltage, where F_d is the position of the steady-state Fermi level at the anode. The ratio of free to trapped carriers is then given by the distribution function, equation 3.3 (a).

By comparing the current where the modified Child's law [3.3 (c)] meets the T.F.L. curve, and the current where the T.F.L. curve meets the Child's law curve [3.2 (b)] the current range of the traps-filled-limit curve is $1/\theta$.

Lampert proposed this theory to explain the results of Smith and Rose (24,37). From equation 3.2 (d) by measuring V_2, it is possible to calculate the trap density. From measuring θ, and using equation 3.3 (a) it is possible to calculate the energy of the trapping level below the conduction band. Thus, if this mechanism is correct, it is a sensitive tool for measuring low trap densities.

The contact limitations discussed in 1.10 have to be borne in mind however, and possible high field effects have to be eliminated when analysing S.C.L. current data.

Skinner (47) has analysed conduction in insulators where diffusion is predominant and Suits (48) has studied insulators with shallow traps. Shockley and Prim (3) have considered trap free insulators. The solutions of equations 3.1 (a), (b), (c) found by these workers are not applicable when deep trapping

states are present.

The theory of Lampert does not explain the phenomena outlined in section 2.6.

3.4 Two-carrier space charge limited conduction in trap free insulators

Two carrier S.C.L. currents have been analysed for trap-free insulators by Parmenter and Ruppel (49). They assumed that diffusion was negligible and recombination between carriers was bimolecular. The basic equations are

$$J = (n\mu_n + p\mu_p)eE \qquad 3.4\ (a)$$

This is a current flow equation, neglecting diffusion.

$$-\mu_n \left(\frac{d}{dx}\right)(nE) = +\mu_p \left(\frac{d}{dx}\right) pE = npvs \qquad 3.4\ (b)$$

This is a continuity equation where v is the thermal velocity of the carriers and s the capture cross-section (1.11).

$$\frac{dE}{dx} = \left(\frac{e}{\epsilon}\right)(n - p) \qquad 3.4\ (c)$$

Poisson's equation

Parmenter and Ruppel concluded that the S.C.L. current is given by

$$J = \frac{9}{8}\,\epsilon\,\mu_{eff}\,\frac{V^2}{d^3} \qquad 3.4\ (d)$$

if the cathode and anode are ohmic for electron and hole flow respectively. The effective mobility μ_{eff} is approximately

$$\mu_{eff} = \frac{2}{3}\left[2\pi(\mu_n\mu_p/\mu_o)(\mu_e + \mu_n)\right]^{1/2}$$

where $\mu_o = \epsilon v S(2e)^{-1}$ and is termed the recombination mobility.

Parmenter and Ruppel estimate the current for two carrier conduction will be enhanced over one-carrier conduction by a factor of the order of 10^3.

This enhancement is due to space-charge neutralisation. It is pronounced in the solid state where the velocity of the carriers is constant. In a vacuum diode, where carriers are continuously accelerated, enhancement factors would only be of the order of 4, ~~even~~ if two carriers of equal masses were assumed.

3.5 <u>Extensions of Lampert and Rose</u>

Rose and Lampert (50,51,52,61) have extended the work of Parmenter and Ruppel to cover general recombination kinetics. Lampert (50), using a simplified approach, shows that for a constant lifetime τ (Recombination through localised centres), which is the same for electrons and holes.

$$J \approx 8\epsilon\tau\mu_n\mu_p \frac{V^3}{d^5} \qquad 3.5\ (a)$$

assuming $\bar{n}$ (3.1) $>$ N_R, the density of recombination centres, and assuming that unneutralised space charge is free. He also derives the results of Parmenter and Ruppel from a simplified approach. He considers field dependent mobilities under the

assumption of a single lifetime for electrons and holes.

Lampert and Rose (51) have considered the more general problem of different electron and hole lifetimes, and have derived 3.5 (a) rigorously. In general terms they predict a square law regime given by

$$J = e\tau\mu_n\mu_p \bar{n} \frac{V^2}{d^3} \qquad 3.5 \text{ (b)}$$

where τ is the average lifetime, followed by a cube law, equation 3.5 (a).

The transition is determined by the time taken for 'relaxation' or neutralisation of injected charge. If the transit time τ_L is greater than the dielectric relaxation time

$$\tau_{RC} = \frac{\epsilon}{e\bar{n}\mu_n}$$

injected space charge is neutralised and 3.5 (b) is valid. When τ_L becomes less than τ_{RC}, injected space charge becomes important and 3.5 (a) is followed.

Lampert (52, 61) has considered the variation of hole lifetime with injection level. He considers an insulator with a single discrete level of recombination centres, N_R, completely filled with electrons in thermal equilibrium. For low injection levels, the electron occupation of the recombination levels remains undisturbed. For high injection levels, recombination empties the levels N_R and effectively

transfers the electrons to the conduction band. The more holes injected, the easier it is for them to cross the insulator in the face of recombination. Lampert predicts that this mechanism will lead to the characteristic illustrated in fig. 3.5.1.

The voltage threshold for two carrier current flow is given by

$$V_{th} = \frac{d^2}{2\mu_p \tau_p \text{ low}} \qquad 3.5\ (c)$$

where τ_p low, is the hole lifetime for low injection levels.

The large increase in hole lifetime can be explained as follows:-

At low injection levels

$$\tau_p \text{low} \approx \frac{1}{v_p \sigma_p N_R}$$

where σ denotes appropriate capture cross-section

At high injection levels, for charge neutrality, $n \approx p$, and the N_R recombination centres are empty, i.e. there are N_R electron traps and

$$\tau_n \approx \tau_p \text{ high} \approx \frac{1}{v_n \sigma_n N_R}$$

and for $\frac{v_p}{v_n} \approx 1$

$$\frac{\tau_p \text{ high}}{\tau_p \text{ low}} \approx \frac{\sigma p}{\sigma n} \quad \text{where } \sigma p \gg \sigma n.$$

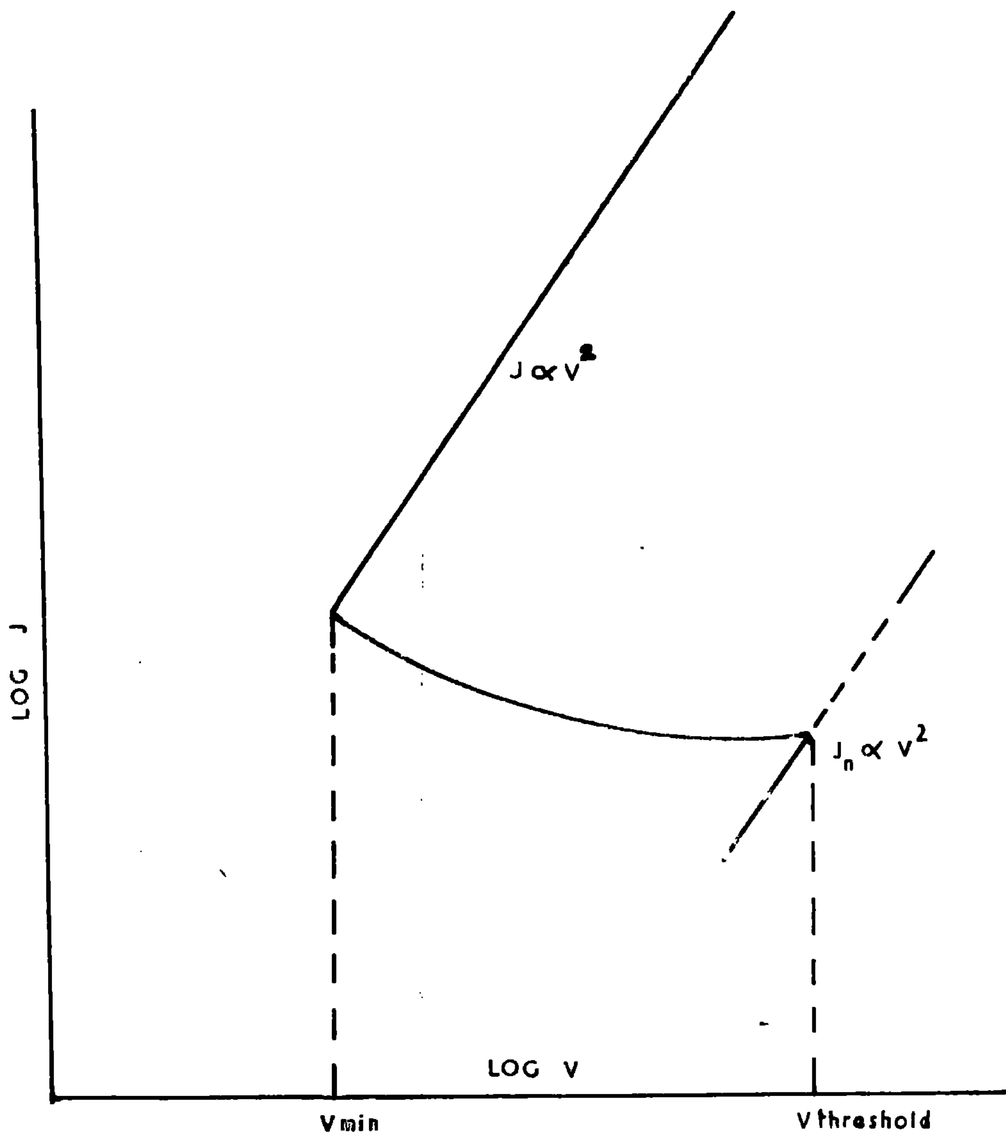

FIG 3.5.1

DOUBLE INJECTION IN INSULATORS — LAMPERT

The upper square law of fig. 3.5.1 is equation 3.5 (b) and the lower square law is Child's law for the trap free insulator (1.9 (a)), with a single carrier.

This analysis hinges on charge neutrality in the crystal. It cannot hold if the injection level is below that for S.C.L. conduction. At low injection levels the characteristic follows Child's law, shown dashed in fig. 3.5.1.

3.6 Photoconductivity in the Gain-Bandwidth product

The gain of a photoconductor can be defined (6) as

$$G = \frac{\Delta I}{eF} \qquad 3.6\ (a)$$

where ΔI is the photocurrent, and F the total number of electron-hole pairs being created per sec. in the photoconductor.

The gain may also be expressed as, the ratio of the free lifetime of a charge carrier, to the transit time between electrodes.

$$G = \frac{\tau_n}{t_n} + \frac{\tau_p}{t_p}$$

The transit time is $t = \frac{d^2}{\mu V}$

thus $$G = (\tau_n \mu_n + \tau_p \mu_p) \frac{V}{L^2} \qquad 3.6\ (b)$$

High photo-conductive gain can be obtained if the lifetime of one of the carriers can be made high. A free carrier can

then make many transits across a crystal before recombining. (This assumes replenishment at the contact.) Gains as high as 10^4 have been observed in cadmium sulphide which are attributed to a very low capture cross-section for free electrons ($\approx 10^{-23}$ cm^{-2}) (15,53,54).

There is no limit from equation 3.6 (b) to the maximum gain of a photoconductor. However it can be shown that the maximum gain of a photoconductor is reached when the photocurrents become comparable with S.C.L. currents.

The maximum gain is given by (55,56,57,52)

$$G_{max} = \frac{\tau_o}{\tau_{RC}} M, \qquad \tau_o = \frac{Nt}{F}$$

where τ_o is the photoconductive decay time or response time of the photoconductor. τ_{RC} is the dielectric relaxation time and $M = \frac{N_A}{Nt}$ where N_A is the number of positive charges on the anode, and Nt is the increment in the total number of photoexcited electrons, free plus trapped, accompanying an increase in the absorbed light flux of amount F. High gain can be achieved at the expense of the response time of a photoconductor and vice versa.

The gain-bandwidth product is

$$G \left(\frac{1}{\tau_o} \right) \doteqdot \frac{1}{\tau_{RC}} \frac{N_A}{Nt} \qquad 3.6\ (c)$$

Nt is a constant dependent only on the electronic structure of the insulator and the intensity of illumination. Space

charge limited conduction occurs when $N_A = Nt$ i.e. when the injected carrier density equals the photo-excited carrier density. Thus M = 1. At voltages above the S.C.L. threshold Nt increases with N_A, thus M has a maximum value of unity.

However if there are localised levels in the forbidden gap which raise the S.C.L. threshold but are not in thermal equilibrium with the free electrons, M can take higher values. Recombination centres are such levels as they are in kinetic rather than thermal equilibrium with the free electrons. M values as high as 500 (33,58,59,60) have been measured.

3.7 Contact controlled response time

Lampert (52) has analysed the response time of a simplified injecting contact, fig. 3.7.1. The current J_o is the steady photocurrent corresponding to some steady level of illumination, and P_o is the position of the potential minimum. On doubling the incident light flux, at constant voltage, the current is approximately doubled to 2 J_o, and the potential minimum moves to P_1.

The time taken for the potential minimum to move from P_o to P_1 is the contact controlled response time τ_{o}, c.

The number of negative charges between P_o and P_1 is

$$Nt_c = \frac{A}{e} (\epsilon kTNt)^{1/2} \qquad 3.7 \text{ (a)}$$

where A is the cross-sectional area and Nt is the total excess charge density at the potential minimum in a simplified diffusion

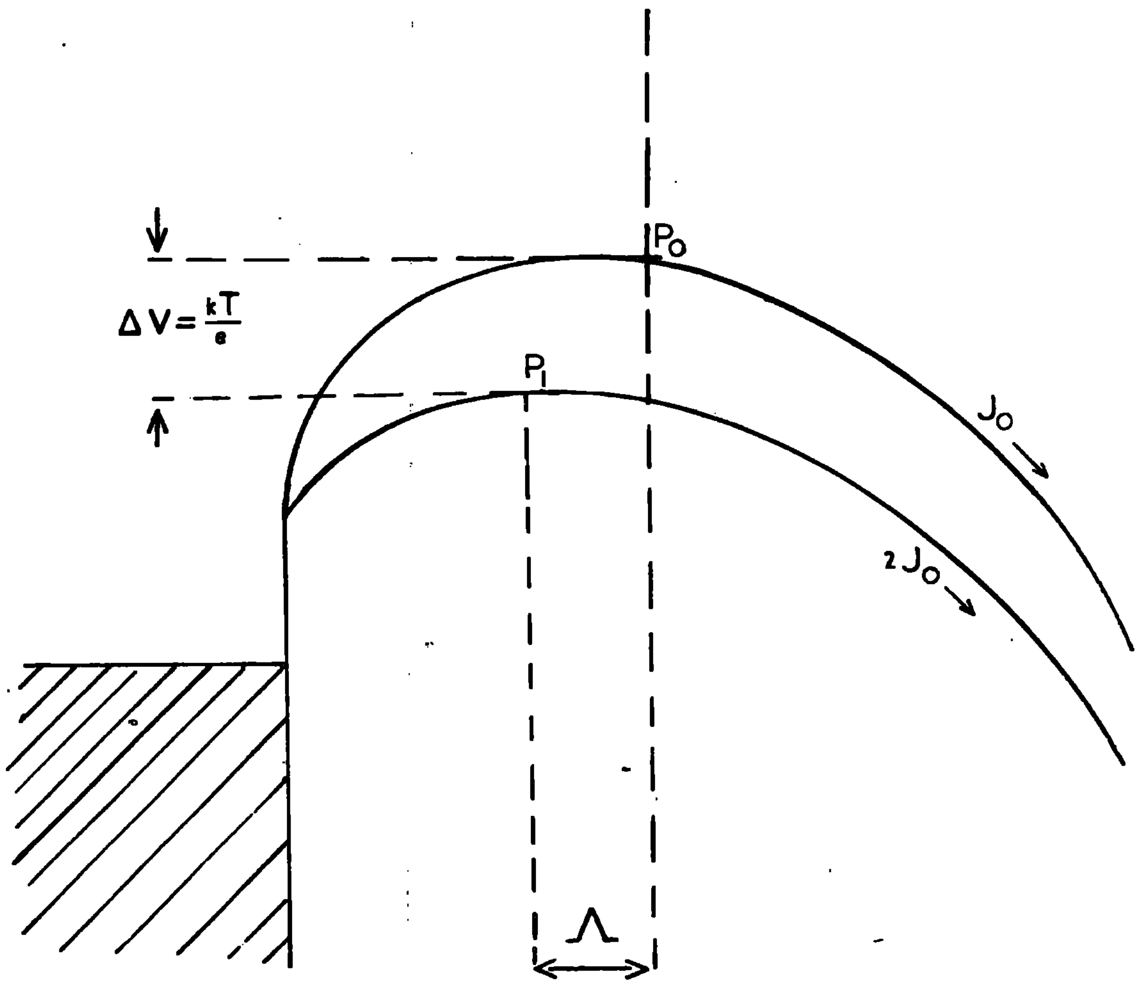

FIG. 3.7.1

TRANSIENT RESPONSE OF AN OHMIC CONTACT

model for the barrier. Λ is the corresponding Debye length and the height of the barrier is reduced by

$$\Delta V \approx \frac{kT}{e}$$

The time taken for the energy barrier to shift from P_o to P_1 is the time taken to build up positive charges to compensate for these additional negative charges and is

$$\tau_{o_c} = \frac{Nt_c}{F} \quad \text{where F is the absorbed light flux} \qquad 3.7\ (b)$$

Lampert therefore concluded that the contact-controlled gain-bandwidth product will be

$$G \frac{1}{\tau_{o\,c}} = \frac{1}{\tau_{RC}} M_c, \qquad M_c = \frac{N_A}{Nt_c}$$

Lampert's derivation is independent of the nature of the current J_o i.e. it can be an ohmic or space charge limited current.

In any given photoconductor, the controlling response time is the longer of τ_o and τ_o.c.

Chapter IV Preparation of Single Crystals of Cadmium Sulphide

4.1. Summary of methods of growth from the vapour phase.

Cadmium sulphide has been prepared from the vapour phase by three distinct techniques.

(i) Combination of the elements

(ii) Chemical transport reaction

(iii) Sublimation of the compound

(i) This is usually termed the Frerich's technique (8,62), and has many modifications (9,63-65). Essentially, cadmium and sulphur(or hydrogen sulphide)are introduced into a hot reaction zone of a furnace as separate vapours. The elements are frequently carried to the reaction zone by an inert gas. Single crystals are formed on the walls of the containing vessel at some cooler portion, usually following the formation of a polycrystalline substrate. Frerich's technique is convenient for growing doped crystals as impurities can easily be added to the carrier gas in controlled quantities during growth.

Woods (76) has investigated the crystal habit under different conditions of growth. Miller and Bachman (66) have produced single crystals of cadmium sulphide by evaporating the elements on to a surface in vacuo.

(ii) Nitsche et al (74,75) have grown cadmium sulphide using iodine to transport the compound down a temperature

gradient in a sealed tube. The cadmium sulphide was transported by way of a gaseous mixture of cadmium iodide and sulphur. A small quantity of iodine was sufficient to transport a large quantity of cadmium sulphide. As the crystals formed the liberated iodine diffused back up the temperature gradient and picked up more cadmium sulphide.

This technique makes growth possible at lower temperatures than (i) or (iii), but by its very nature is only suitable if traces of iodine can be tolerated in the final crystals.

(iii) Cadmium sulphide can be sublimed and recrystallized, either in a sealed tube (67-72), or with the assistance of a carrier gas (73). As in (i), there are many modifications. Fochs, for example, varied the temperature gradient during growth and grew isolated single crystals on the wall of a silica tube. Generally, the compound is maintained at some maximum temperature, sublimation occurs, and recrystallization in the cooler portions of the system produces single crystals. In our laboratory a sublimation technique has been found to be more convenient for growing plate-like crystals suitable for space charge limited current measurements.

We have used three methods to grow single crystals of cadmium sulphide. The experimental parameters to be described are typical of the above three divisions.

4.2. Preparation by combination of the elements

Cadmiüm sulphide crystals were grown using apparatus

illustrated in fig. 4.2.1. The silica tube measured 90 cms by 2.6 cms bore and was placed in a two zone furnace. The temperature distribution along the silica tube is illustrated in fig. 4.2.1. The transport of cadmium and sulphur vapour to the reaction zone was controlled by varying the position of the cadmium boat and the sulphur pipette, and by adjustment of the separate flows of argon. Single crystals grew, after the formation of a polycrystalline substrate, on the wall of the silica tube.

Difficulty was experienced in the control of the separate flows of vapour, and the crystals grown were predominantly hexagonal rods. The sublimation method was therefore investigated. This is described in section 4.4.

4.3. Preparation by iodine transport

Single crystals have also been prepared by an iodine transport technique. A small quantity (estimated at < 1 mg) of iodine was condensed under vacuum into a silica tube containing 2.5 grams of cadmium sulphide powder. The tube measured 20 cms by 1 cm bore and was sealed off under vacuum. The system was placed in a furnace with a uniform temperature gradient of 970 - 770°C extending down the tube. The powder was at the higher temperature. After seven days the powder had been transported down the temperature gradient and single crystals had grown on an area of the wall that had been at 800°C.

Further experiments, designed to grow crystals by this

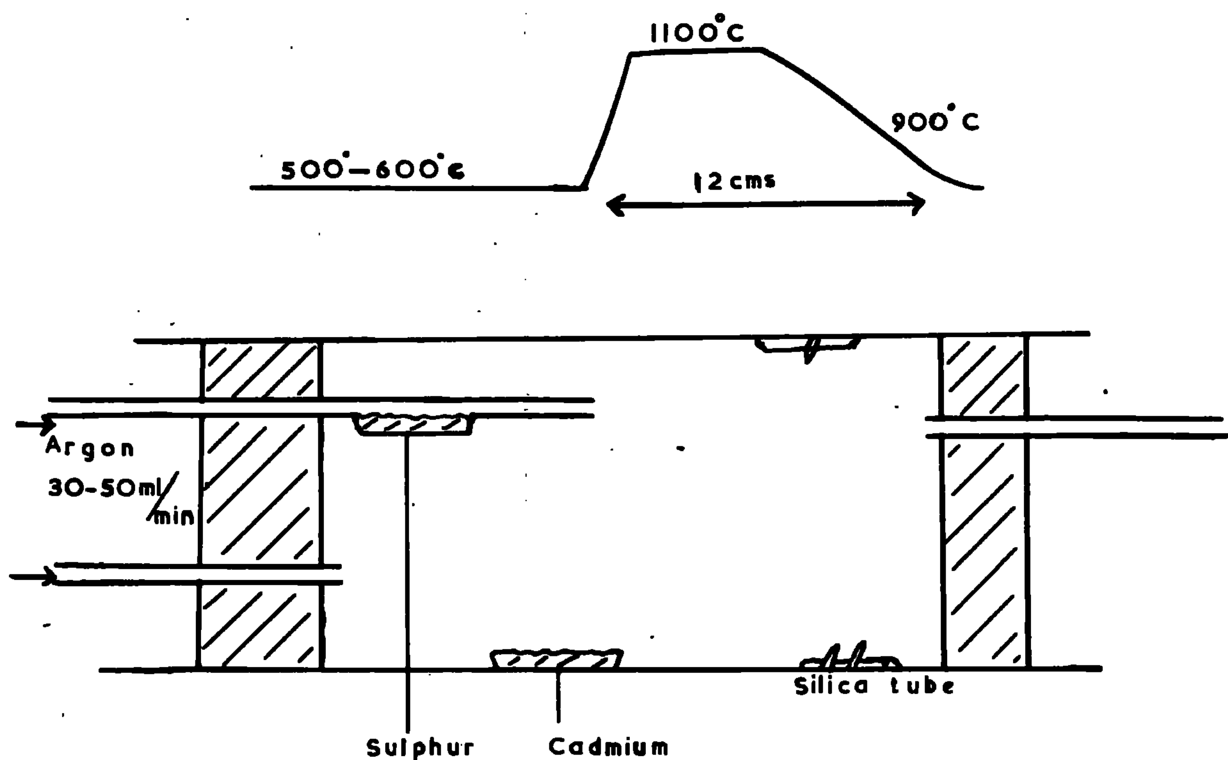

FIG. 4.2.1.

TEMPERATURE PROFILE AND EXPERIMENTAL ARRANGEMENT FOR GROWTH BY COMBINATION OF THE ELEMENTS.

method in tubes with larger bore, have so far proved unsuccessful. The crystals were hexagonal rods and not suitable for space charge limited current measurements.

4.4. <u>Preparation by sublimation of the compound</u>

The apparatus used is illustrated in fig. 4.4.1. The sublimation was effected in a silica tube (90 cms by 2.6 cms bore) fitted with transparent ends to observe the crystal growth. The powdered compound was supplied by Light and Company and was degassed at 500°C in vacuo, for 3 hours, before use. The furnace was heated by four silicon carbide elements symetrically placed about the bore. The electrical circuit is illustrated in fig. 4.4.2. The Ether controller maintained the maximum temperature constant to ± 6°C. There was an approximately linear temperature gradient of 250°C in 10 cms at either side of the maximum temperature.

The sublimation was assisted by a stream of high purity argon (99.995% W/V), which was passed over copper maintained at 400°C in a subsidiary furnace. This was to remove traces of oxygen. The argon flow was then passed through a molecular drier, monitored by a flowmeter, and finally passed into the silica tube.

Before growth the silica tube was flushed with argon, and the flow was maintained until the whole apparatus was returned to room temperature.

Optimum growth (i.e. a maximum number of thin clear plates)

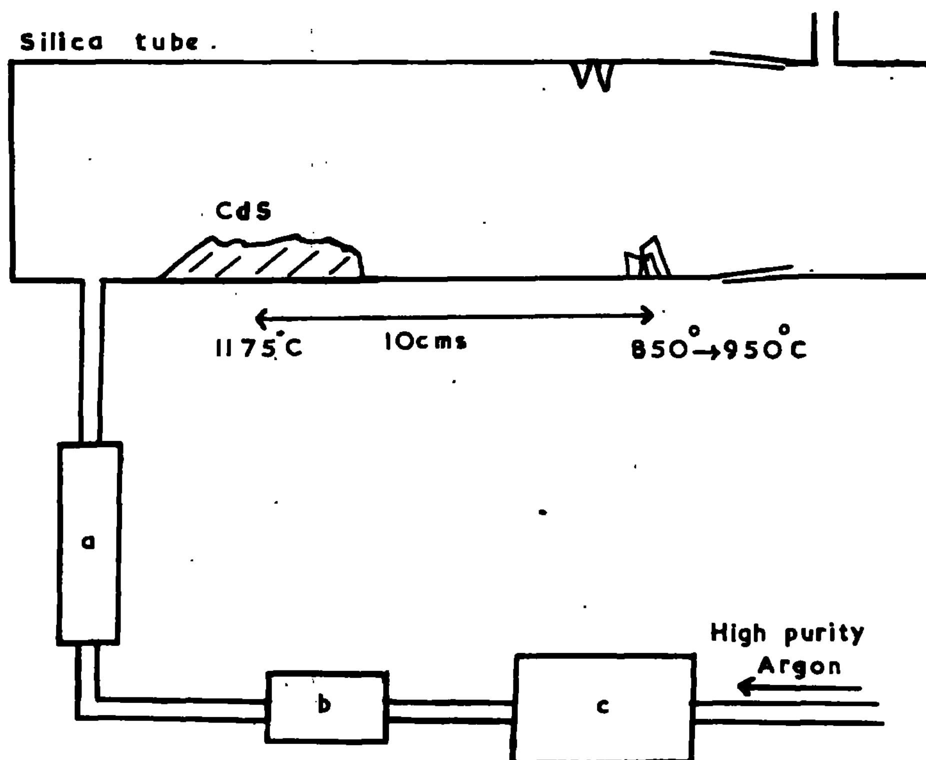

a Flowmeter

b Drying tower (Aluminium Calcium Silicate.)

c Copper at 400°C

Not to scale.

FIG. 4.4.1.

PREPARATION BY SUBLIMATION OF THE COMPOUND.

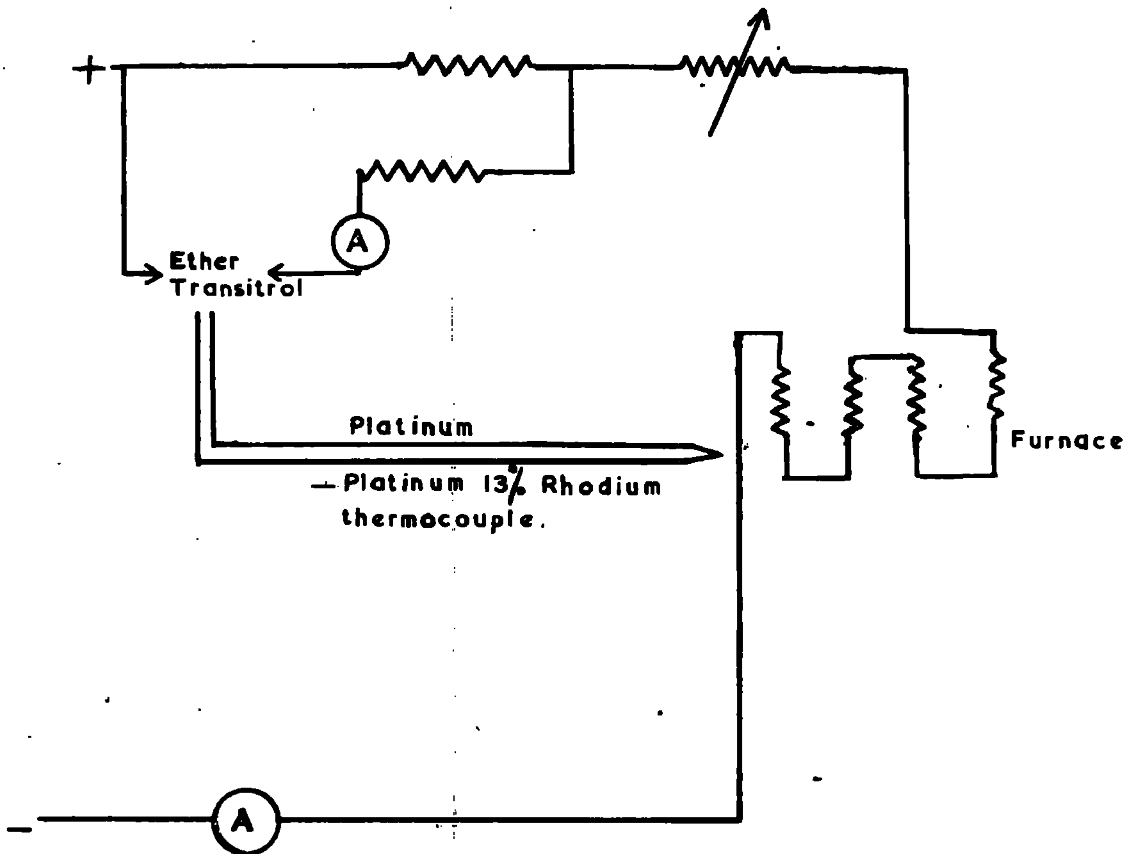

FIG. 4.4.2.

FURNACE CONTROL CIRCUIT

was obtained with a flow of 180-190 mL/min and a charge temperature of 1175°C. The crystals were formed at temperatures between 850 and 950°C. The maximum temperature was maintained for between 65 and 75 minutes. This growth time was critical.

The dimensions of the plates were of the order 5 x 4 x 0.02 mms. They displayed edge emission (2.1) on excitation with an ultra violet lamp at liquid air temperatures. Some plates showed surface striations parallel to the long axis of the plate. Only crystals free from these defects were selected for experimental study.

4.5 General observations on the sublimation growth of cadmium sulphide

Plate-like crystals grew directly on the walls after the formation of a thin substrate, or on, but not from, fine needles which grew within 30 minutes of the charge reaching the growth temperature. Towards the cooler end of the tube, thicker plates were grown which consisted of several laminated sheets of cadmium sulphide. Thin crystals could sometimes be obtained by cleaving a crystal of this type. Towards the hotter portion of the silica tube (closer to the charge), the thin needles tended to grow into hexagonal rods. Once the tube was partially filled with fine needles the thin clear plates grew rapidly. If growth was maintained for longer than 75 minutes, only thick plates were obtained. If the growth was maintained for less than 65 minutes, few plates were grown. A typical run produced

between two and three dozen suitable crystals.

Fluctuations in the argon flow produced wispy growth which rapidly blocked the tube, few plates being formed.

Water vapour deliberately included in the argon flow had little effect on the crystal growth. The resultant crystals displayed intensified edge emission and at temperatures above liquid air, a red component was observed which was not apparent in the pure crystals.

Oxygen in the system enhanced crystal growth. Plates greater than 1 sq. cm. were grown but had a number of striations on both surfaces. The plates were grown from rods, and could be grown at flow rates as low as 30 mL/min. Crystals grown under these conditions did not display edge emission. By annealing in cadmium sulphide powder for 2 hours at 700°C in vacuo, the crystals could be made to exhibit edge emission to a variable degree.

Crystals grown with oxygen present had a resistivity of the order of 10^8 ohm. cm. Crystals grown either with water vapour present or in the pure form, had resistivities of the order of 10^{12} ohm. cm.

4.6 Conclusions

With the sublimation technique, a combination of steep temperature gradient and high argon flow favours the growth of plate-like crystals. This indicates that a high supersaturation at the point of recrystallization favours this crystal habit.

A detailed study would require precise knowledge of the local temperature and supersaturation to determine the conditions producing the two distinct habits observed. The sublimation technique, however, was satisfactory for growing crystals of the desired dimensions and purity. The effect of oxygen on the growth and properties of single crystals of cadmium sulphide needs further investigation.

Bube (77) has investigated the effect of water vapour on the photoconductive properties of cadmium sulphide.

Chapter V Apparatus, experimental procedures and results

5.1. Contact materials and methods of application

Indium, graphite, silver, gold and copper were used as contacts on the platelets of cadmium sulphide.

The electron injecting contact, or cathode, was provided by indium (section 2.2). The indium was applied by the following three methods:

(i) Soldering to the crystal in air (melting point 115°C).

(ii) Evaporating the indium on to the crystal using an Edwards model 6E coating unit.

(iii) Placing an indium bead on the surface of the crystal and then heating in argon to 300°C for 3 minutes.

No special cleaning of the crystal surfaces was given when methods (i) and (iii) were used. However, before applying indium by evaporation (ii), the surface of the crystal was cleaned by 2keV electron bombardment or by ionic bombardment in hydrogen. This was done in the coating unit prior to evaporation.

Contacts produced by method (i) were not satisfactory. The current-voltage characteristics were erratic and irreproduceable. This technique was abandoned. Cathode contacts applied by (ii) or (iii) gave steady reproduceable results.

Two types of anode contact were used: Indium, which would be expected to provide a hole blocking anode, and

several high work function contacts as hole injecting anodes. (section 2.3).

The indium anodes were made by the techniques described in (ii) and (iii). Evidence will be presented that anodes prepared by (iii) are not hole blocking contacts.

Silver and graphite were applied to the crystals by painting on colloidal dispersions of these materials obtained from Acheson Colloidals Limited. Evaporated silver, gold and copper anodes were also employed. Graphite was used for the majority of the experiments where a hole injecting anode was required.

The contacts and methods of application used are indicated for the individual experiments. The conclusions which can be drawn concerning the different contacts are contained in the following chapter.

5.2. Direct current-voltage characteristics at room temperature

The current-voltage characteristics were measured with a vibrating reed electrometer and associated current measuring unit. (Vibron models 33B and A33B). The voltage applied to a crystal was derived from batteries. The current was determined by observing the voltage developed across the appropriate high resistance of the current measuring unit in series with the crystal. The circuit is illustrated in fig. 5.2.1. The current measuring unit contained resistances of 10^6, 10^8 and 10^{10} ohms. The input impedance of the

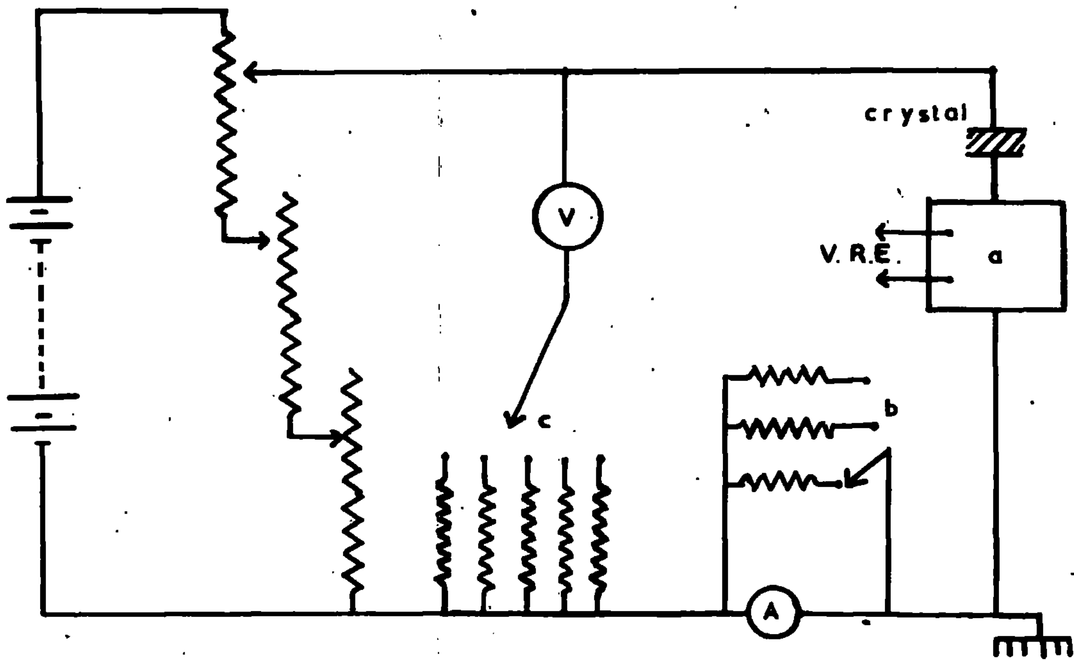

a. current measuring unit.

b. switch ranges, 100μA 1mA and 10mA f.s.d.

c. switch ranges 0·2, 1, 10, 100, 200volts f.s.d.

FIG. 5.2.1.

CIRCUIT FOR DIRECT CURRENT—VOLTAGE CHARACTERISTICS.

electrometer was 10^{13} ohms. This apparatus enabled currents from 10^{-13} to 10^{-2} amperes to be measured with applied voltages of up to 200 volts across the crystal.

The crystal was mounted on a microscope slide in a light proof metal box. Connection to the top of the crystal was made via a phosphor bronze spring wire to one of two bulldog clips holding the slide. The bottom connection was made via the other bulldog clip. The metal box provided a good electrostatic screen for the crystal, and good insulation was obtained by isolating the bulldog clips from the casing with polytetraflouroethylene (P.T.F.E.) washers. The crystal mount is shown in fig. 5.2.2.

On initially applying a voltage, a high current was observed. This current decreased over a period of several minutes to a low steady value. For a crystal with soldered indium contacts, or a crystal grown in the presence of traces of oxygen, several hours were required before the current decreased to a stationary reproduceable value.

In the work described in this section, all the indium contacts were made by heating the indium and crystal in argon to 300°C for 3 minutes.

A typical current-voltage characteristic for a cadmium sulphide crystal with two indium contacts is shown in fig. 5.2.3. Three regions are apparent. An Ohm's law region at low voltages, followed by a steep rise in current and finally a second Ohm's law region. These three parts are marked

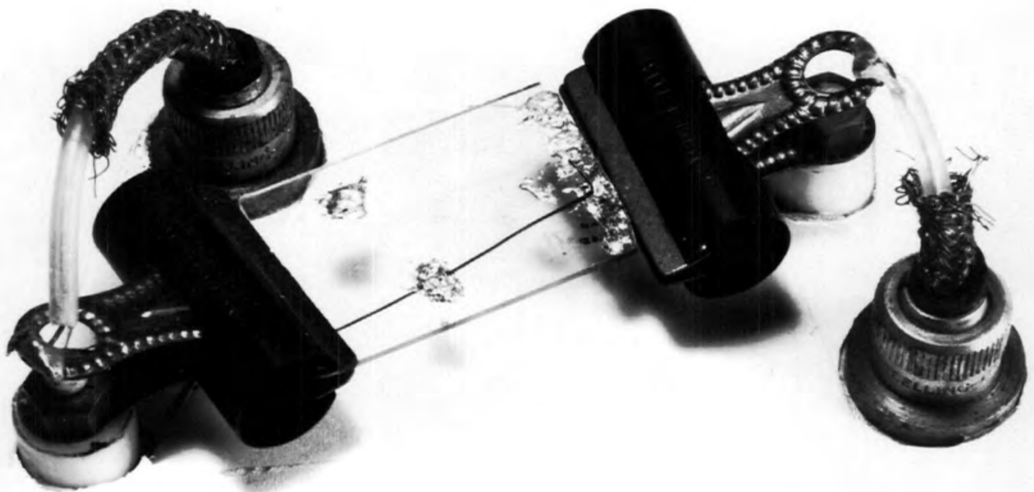

FIG. 5.2.2.

METHOD OF MOUNTING CRYSTALS FOR ROOM TEMPERATURE MEASUREMENTS.

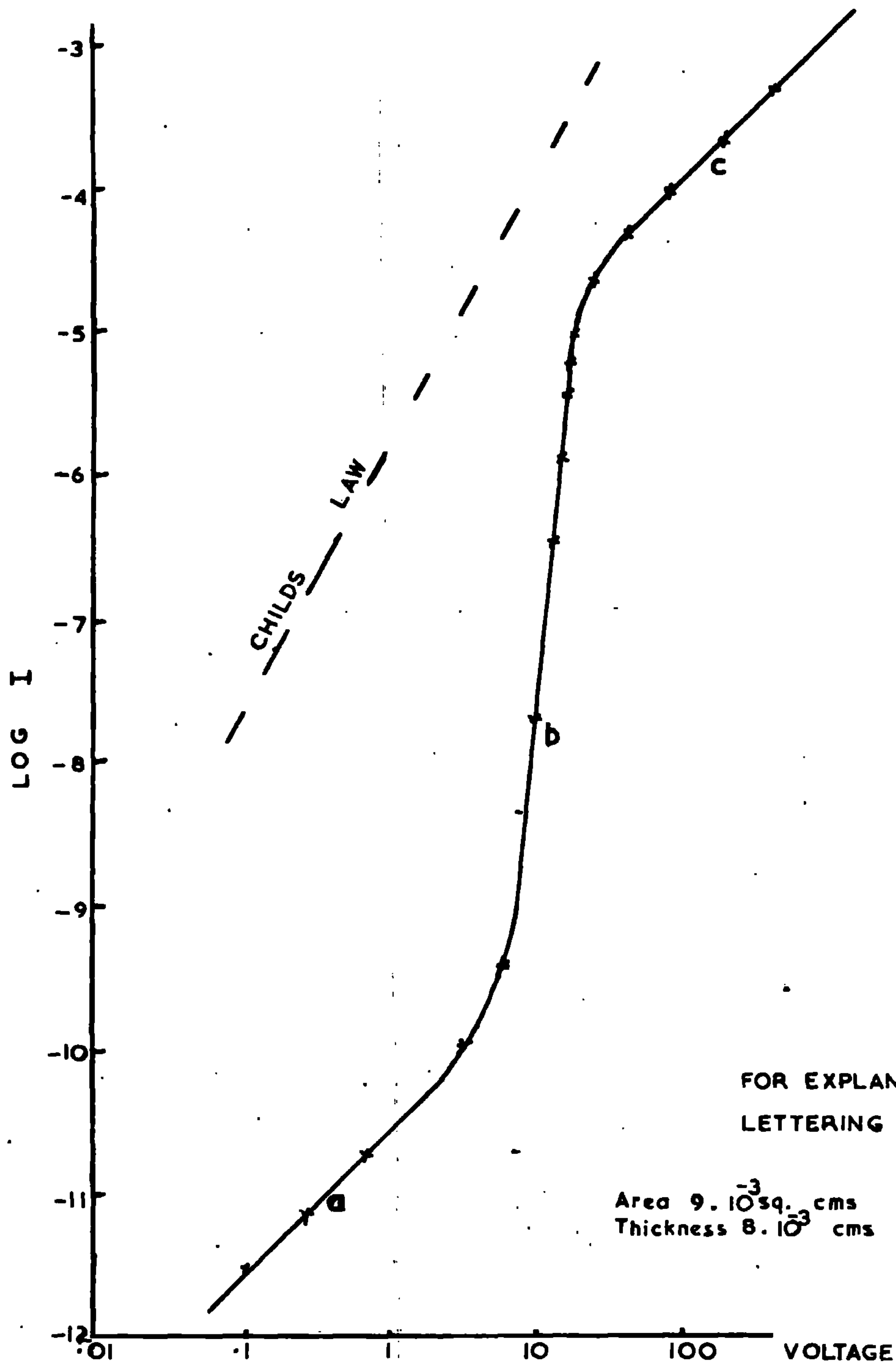

FIG 5.2.3.

CHARACTERISTIC OF A CRYSTAL
WITH TWO INDIUM
CONTACTS

a,b,c on fig. 5.2.3., respectively. Some crystals did not show an Ohm's law region at high voltages. The current would increase in these crystals, (in a manner similar to region b) until the crystals suffered an irreversible breakdown. The expected square law at high voltages was not observed for crystals with two indium contacts. The Ohm's law regime at high voltages, indicates that the contacts were saturated at these voltages.

The current-voltage characteristic of a crystal with an indium cathode and graphite anode is shown in fig. 5.2.4. The characteristic can be divided into four regimes. An ohmic part 'a', followed by a steeply rising portion 'b'. This in turn is followed by a negative resistance region 'c', and by a square law region 'd'. The square law region at high voltages was not always observed. Some crystals obeyed Ohm's law at high voltages while others suffered an irreversible breakdown. The high current end of the characteristic for these cases is shown in fig. 5.2.4. by the dotted lines e and f respectively. The negative resistance regime was completely reproduceable. At liquid air temperatures, luminescence very similar to edge emission was observed in crystals exhibiting this behaviour. On reversing the voltage applied to a crystal with a graphite anode a rectification ratio greater than 10^5 was observed with applied voltages up to about 20 V. The reverse current followed Ohm's law.

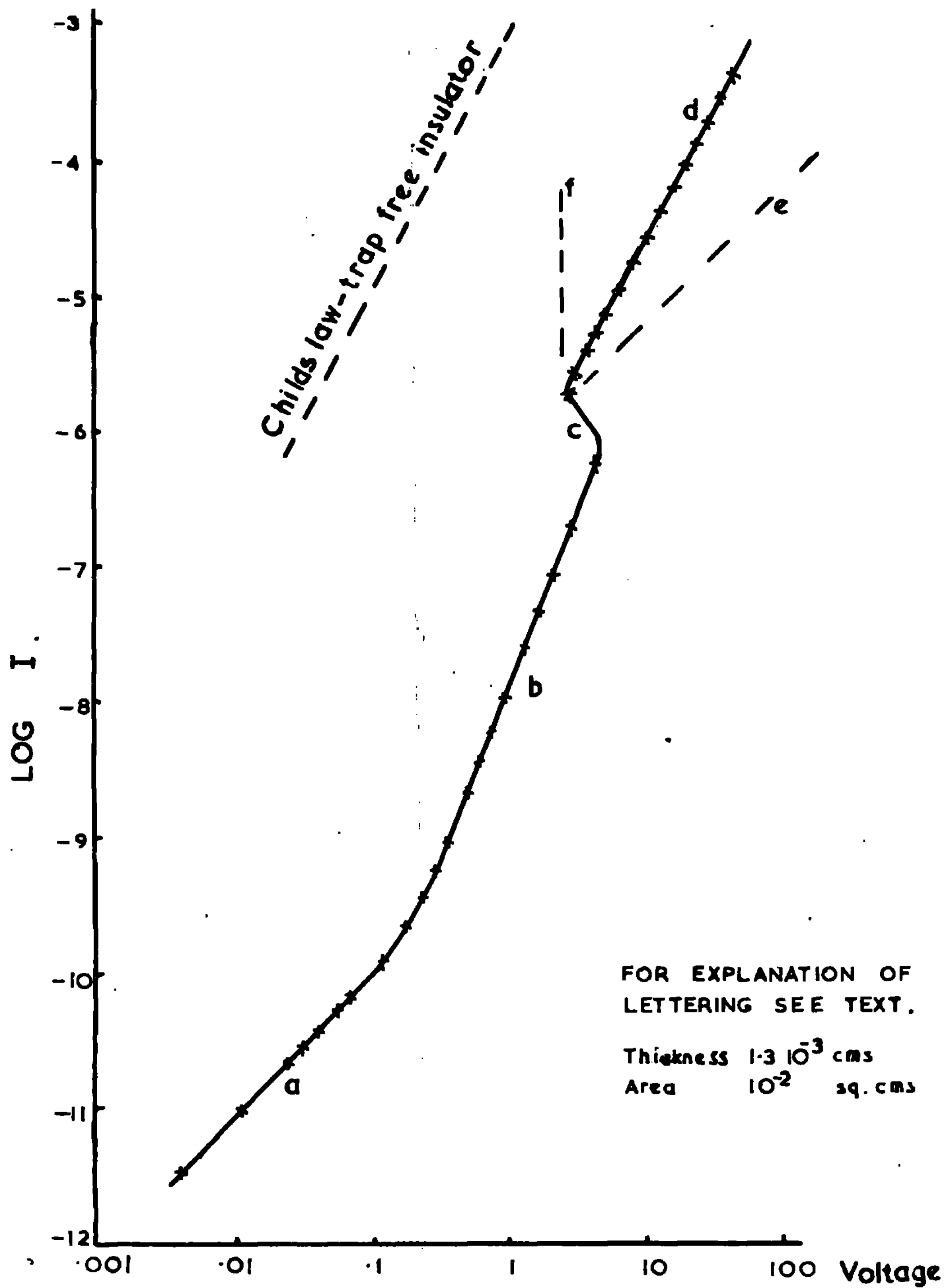

FIG 5.2.4.

CHARACTERISTIC OF A CRYSTAL WITH AN INDIUM CATHODE AND A GRAPHITE ANODE

This aspect, however, was not pursued.

A negative resistance region was observed in the characteristics of two crystals with indium anodes of type (iii). One of these characteristics is shown in fig. 5.2.5. The negative resistance region was more apparent than in crystals with graphite anodes.

5.3. Temperature variation of direct current-voltage characteristic.

The current-voltage characteristic of a crystal with two indium contacts has been measured at eight different temperatures. The contacts were applied by evaporation. The electrical circuit was that described in section 5.2. The crystal was contained in a copper cryostat which is shown in fig. 5.3.1. The crystal was mounted on a microscope cover slip. The cover slip was held against a central block of copper by phosphor bronze spring wires which made the electrical connections to the indium. The mounted crystal can be seen in fig. 5.3.1. The temperature of the central copper block, and hence the crystal temperature, was varied by inserting freezing mixtures in the inner vertical tube of the metal dewar. The temperature could be raised above ambient by a heater, which is shown in position in the inner tube. The heater was totally enclosed in a silica jacket. The two vertical tubes were of german silver to reduce temperature losses. The outer tube acted as a vacuum jacket and was

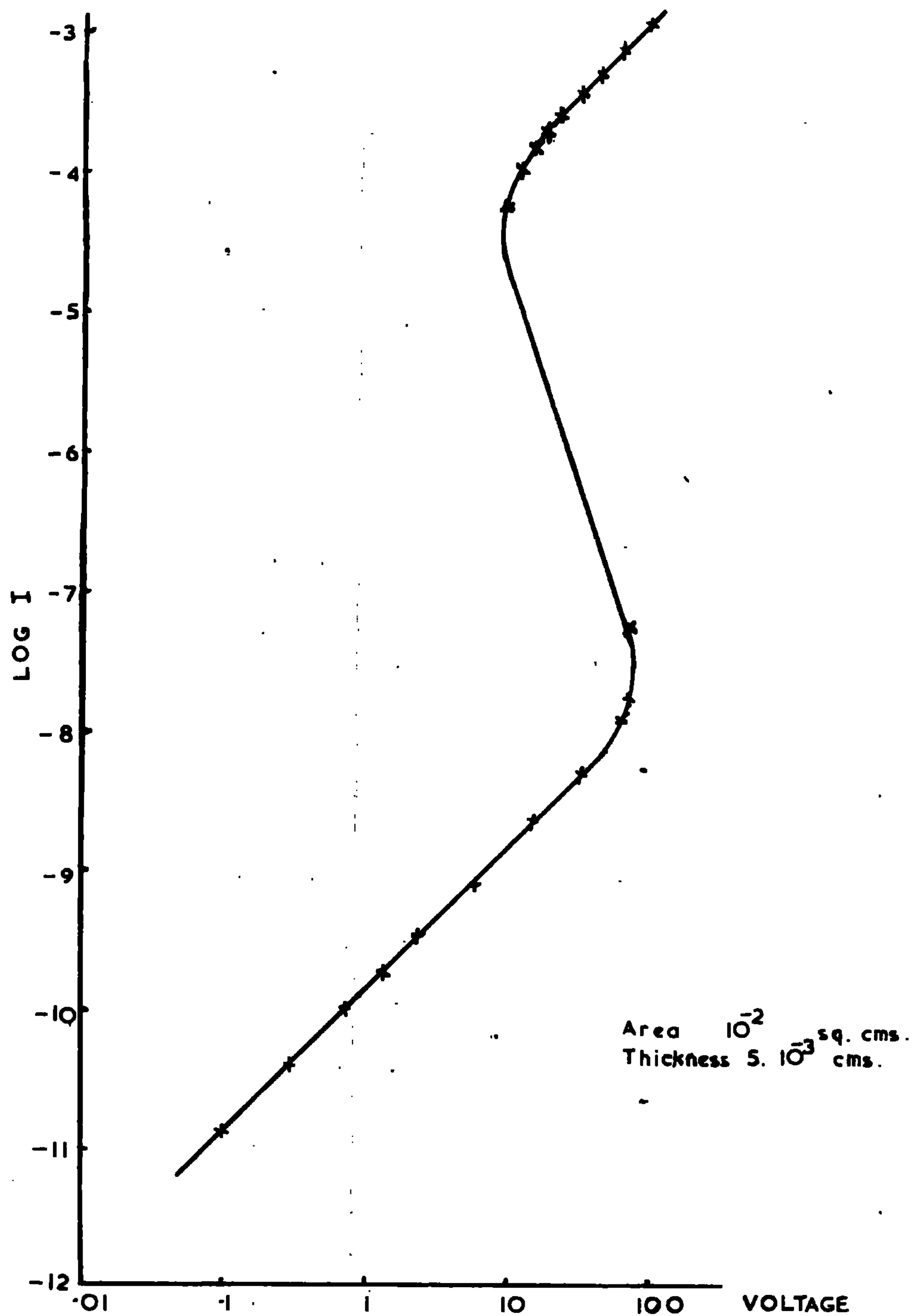

FIG 5.2.5.

CHARACTERISTIC OF A CRYSTAL WITH TWO INDIUM CONTACTS

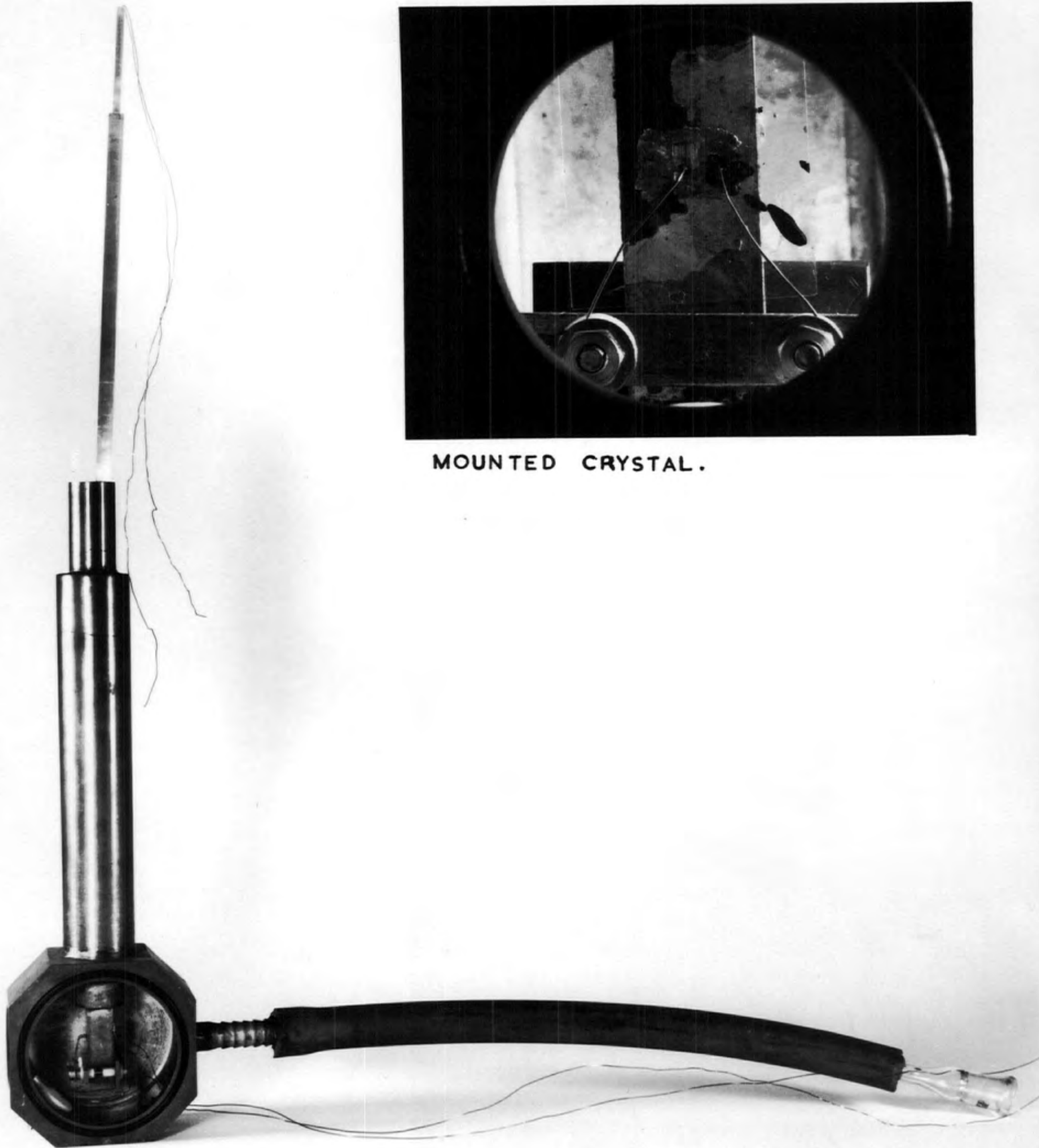

MOUNTED CRYSTAL.

FIG. 5.3.1.

CRYOSTAT FOR TEMPERATURE MEASUREMENTS.

soldered to the outer walls of the cryostat. The inner tube was hard soldered to the copper block which was bored out to receive the freezing mixtures, and the heater. The inner tube was held by soldering it to the top of the outer tube, the space between the two tubes being evacuated. Electrical connections to the crystal, and thermocouple leads, entered via metal-glass four way seals. Difficulty was experienced in excluding light that entered through these seals. Plugs of P.T.F.E., one of which can be seen in fig. 5.3.1., were used to reduce photo effects and provided the cryostat was not exposed to direct light these were satisfactory. Access to the cryostat was possible via two holes, one in the side of the cryostat and one facing the crystal. Vacuum seals between the cryostat and the covers for the holes (not shown in fig. 5.3.1.), were made using O-rings set in the two faces of the cryostat. A photomultiplier could be fitted in place of the cover facing the crystal. The terminals, holding the phosphor bronze wires, were insulated from the strips of copper holding them to the central block by P.T.F.E. washers. Silicon vacuum grease served to improve thermal contact between the cover slip and the copper block. In a preliminary experiment the temperature drop between the copper and the crystal was found to be less than 5°C. It was not possible to measure the temperature of the crystal directly during the course of the main experiment due to the high

standard of insulation required. The thermocouple was therefore connected to the central block and this was taken to be the temperature of the crystal.

Temperatures below room temperature were obtained by inserting four cooling agents in the inner vertical column of the cryostat. They were, in order of increasing temperature, liquid air, solid carbon dioxide in acetone, melting carbon tetrachloride and melting ice. Temperatures above ambient were obtained using the resistance heater. The heater was immersed in water to aid thermal contact with the central block of copper.

Before taking each set of readings the crystal was shorted to earth and heated to 100°C for several minutes to remove excess charge trapped in the crystal.

The results of this experiment are presented in fig. 5.3.2. In order to avoid possible damage to the crystal the characteristic was not measured beyond the steeply rising portion.

5.4. <u>Current-voltage characteristics using pulsed fields</u>

Pulsed voltages were applied to crystals with two indium contacts and to crystals with indium cathodes and graphite anodes. The indium contacts were made by heating the indium and crystal in argon to 300°C for 3 minutes.

The pulses were derived from a Nagard model 5002 pulse generator. The length of the pulse was variable from 0.2μ secs to 2 secs, the repetition frequency ranged from 0.1 c.p.s. to

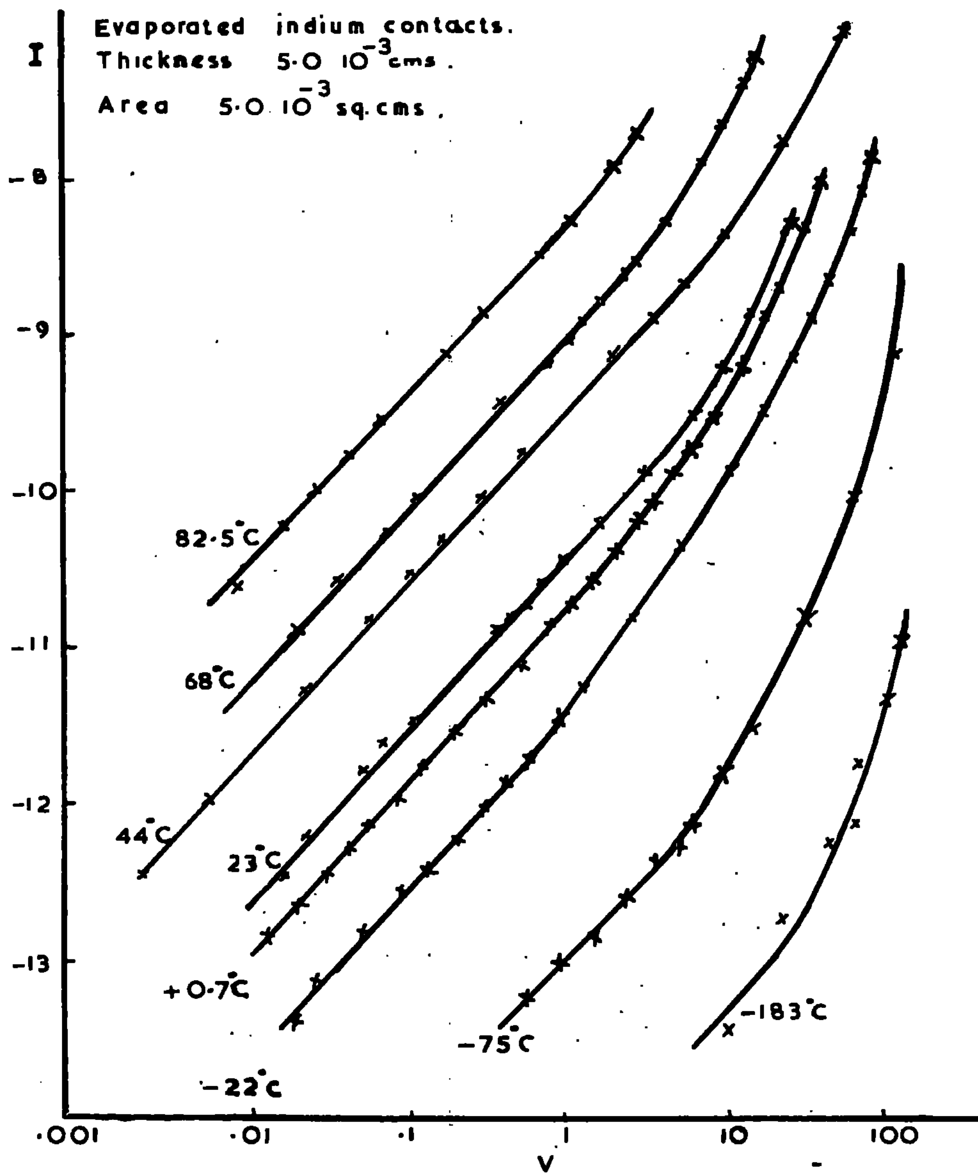

FIG. 5.3.2.

LOG—LOG PLOT OF THE

CURRENT—VOLTAGE CHARACTERISTIC

AT DIFFERENT TEMPERATURES

1000 kc.p.s. and the available voltage from 20mV to 50V. The current waveforms were observed on a Tektronix 545A oscilloscope with a type CA plug-in unit. The input impedance was 10^6 ohms and the maximum sensitivity 0.05v/cm. The voltage developed, across a resistance in series with the crystal, gave a measure of the form and magnitude of the current through the crystal.

No significant differences were observed between crystals with indium contacts, and crystals with an indium cathode and graphite anode. On reversing the sign of the voltage applied to the latter crystals, (i.e. making the graphite the cathode), rectification was observed. The reverse currents were too small to measure with the available apparatus and no estimate of the rectification ratio could be made.

In the forward direction the current-voltage characteristic followed Ohm's law up to some voltage, and thereafter followed a cube law. This is illustrated by the example in fig. 5.4.1. The crystals were mounted in the light proof box, in the manner described in section 5.2. The characteristic is that obtained by measuring the initial current flowing through the crystal.

For pulses shorter than 5ms, and with low voltages, the shape of the current pulse was as shown in fig. 5.4.2.(a). At higher voltages, the end of the pulse was abruptly raised, giving a current pulse similar to that illustrated in

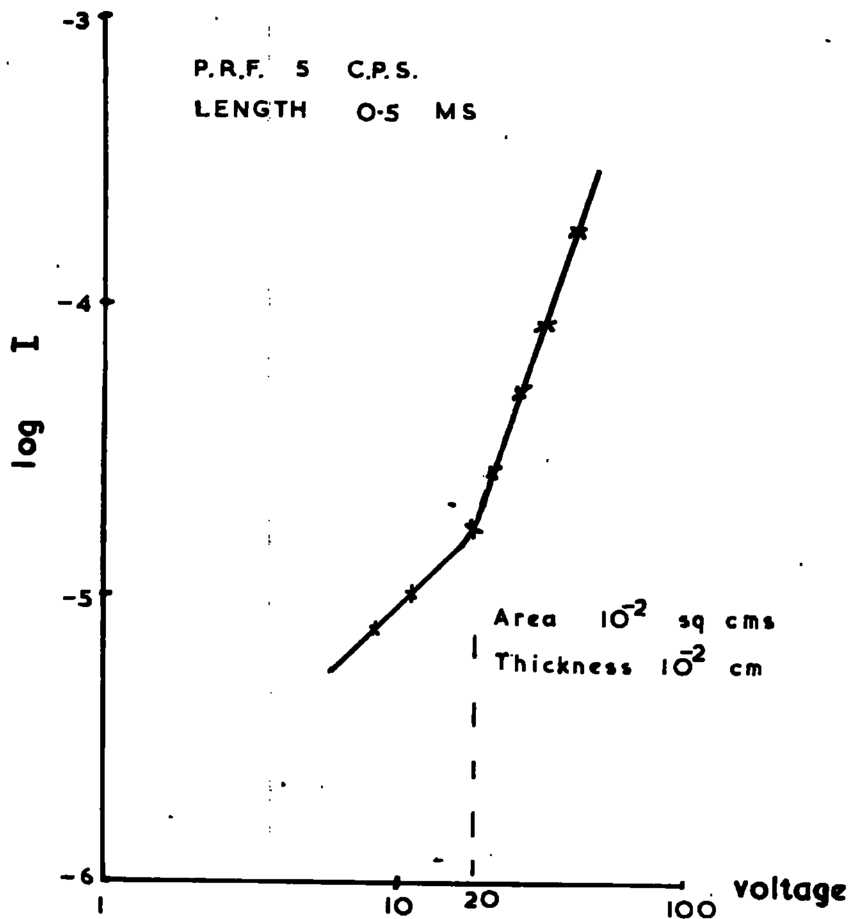

FIG 5.4.1.

CHARACTERISTIC UNDER PULSED FIELDS

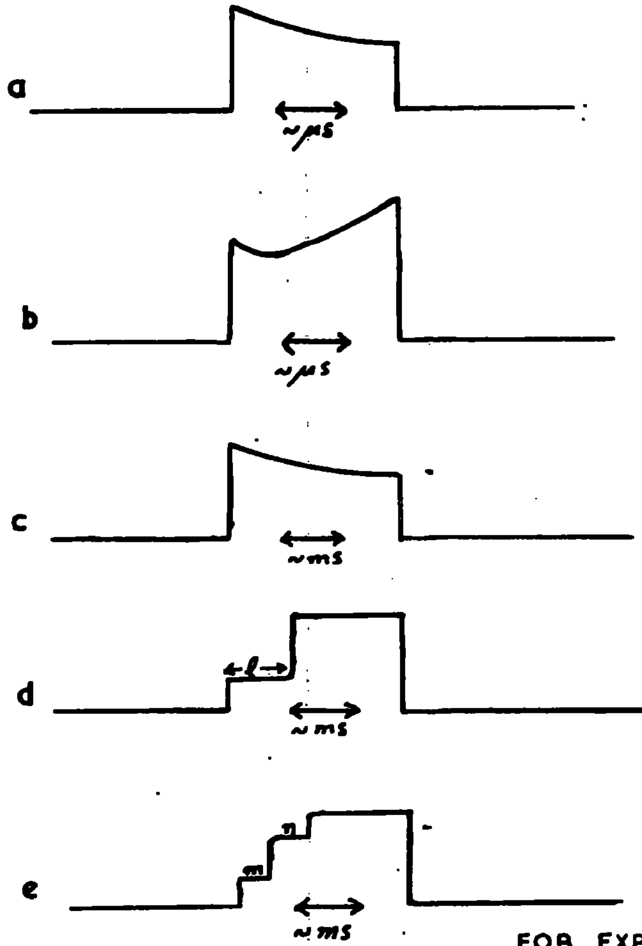

FIG 5.4.2

TYPICAL CURRENT PULSES

fig. 5.4.2. (b). This would generally occur with of the order of 40 volts across a crystal approximately 10^{-2}cms thick.

For pulses longer than 5ms, and at low voltages, the current pulse was similar to that of fig. 5.4.2.(c). For these current pulses, the following empirical relation was found to be obeyed:-

$$I = I_o e^{-t/t + x} \qquad 5.4. (a)$$

where I_o and I are the initial and final currents, t is the length of the pulse and x is of the order of 4ms. This relation was obeyed for pulse lengths between 5 and 30ms.

At higher voltages, the discontinuity illustrated in fig. 5.4.2. (d) was observed in the current pulse. On raising the voltage above some threshold, the end of the current pulse would be raised. The length of the current pulse ℓ, before the sharp rise in current, depended on the applied voltage. The higher the applied voltage, the shorter the length of the plateau ℓ.

Two transient effects were also observed. On increasing the voltage or P.R.F., the current pulse would sometimes be of the form shown in fig. 5.4.2.(e). After the application of several voltage pulses, the current pulse would revert to that shown in fig. 5.4.2.(d). The lengths of the two plateaus (m,n, fig. 5.4.2.(e)) varied for successive pulses. The second

transient effect was also observed on initially increasing the voltage or P.R.F. On increasing either of these, the length of the plateau (ℓ , fig. 5.4.2.(d)), would initially be unaffected. However successive pulses would decrease the length of ℓ, until, after the application of several pulses at the higher P.R.F. or voltage, the length ℓ would settle to a new, consistently smaller value. The reverse of this second transient effect was also observed. On decreasing the voltage or P.R.F., the length ℓ increased over successive pulses to a consistent value.

The voltage required to produce the discontinuity illustrated in fig. 5.4.2 (d) depended on the pulse repetition frequency according to:

$$\text{P.R.F.} = \alpha \, e^{-\beta V} \qquad 5.4.\,(b)$$

where α and β were different constants for different pulse lengths.

The length of the current pulse ℓ , before the current discontinuity, was related to the pulse repetition frequency by

$$\ell = \gamma \, e^{-\delta(\text{P.R.F.})} \qquad 5.4.(c)$$

where γ and δ were constant. This was determined for a pulse length of 100ms.

The two relationships are illustrated graphically in fig. 5.4.3. and fig. 5.4.4. respectively.

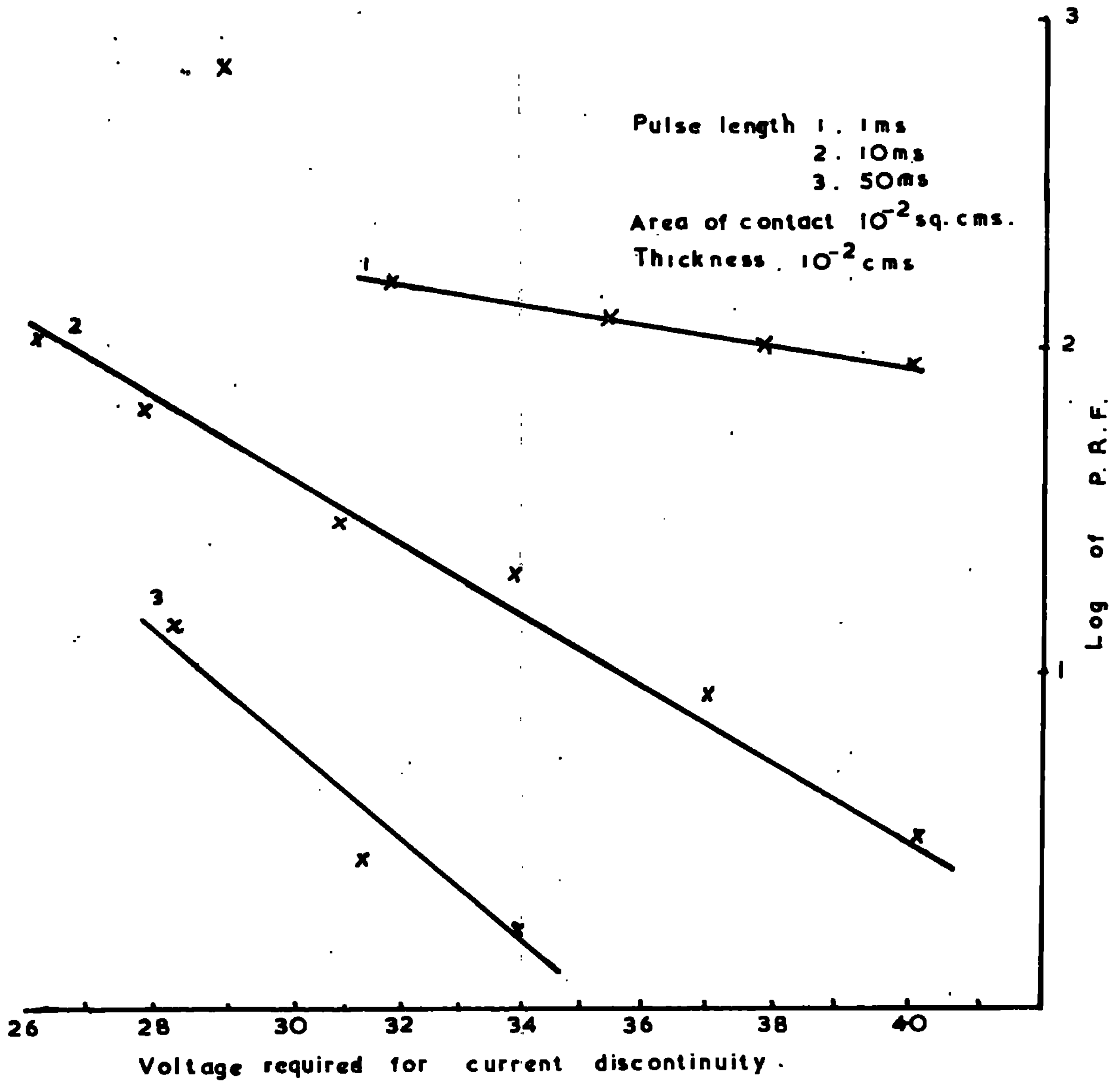

FIG. 5.4.3.

VOLTAGE—P.R.F. RELATIONSHIP TO ESTABLISH CURRENT DISCONTINUITY.

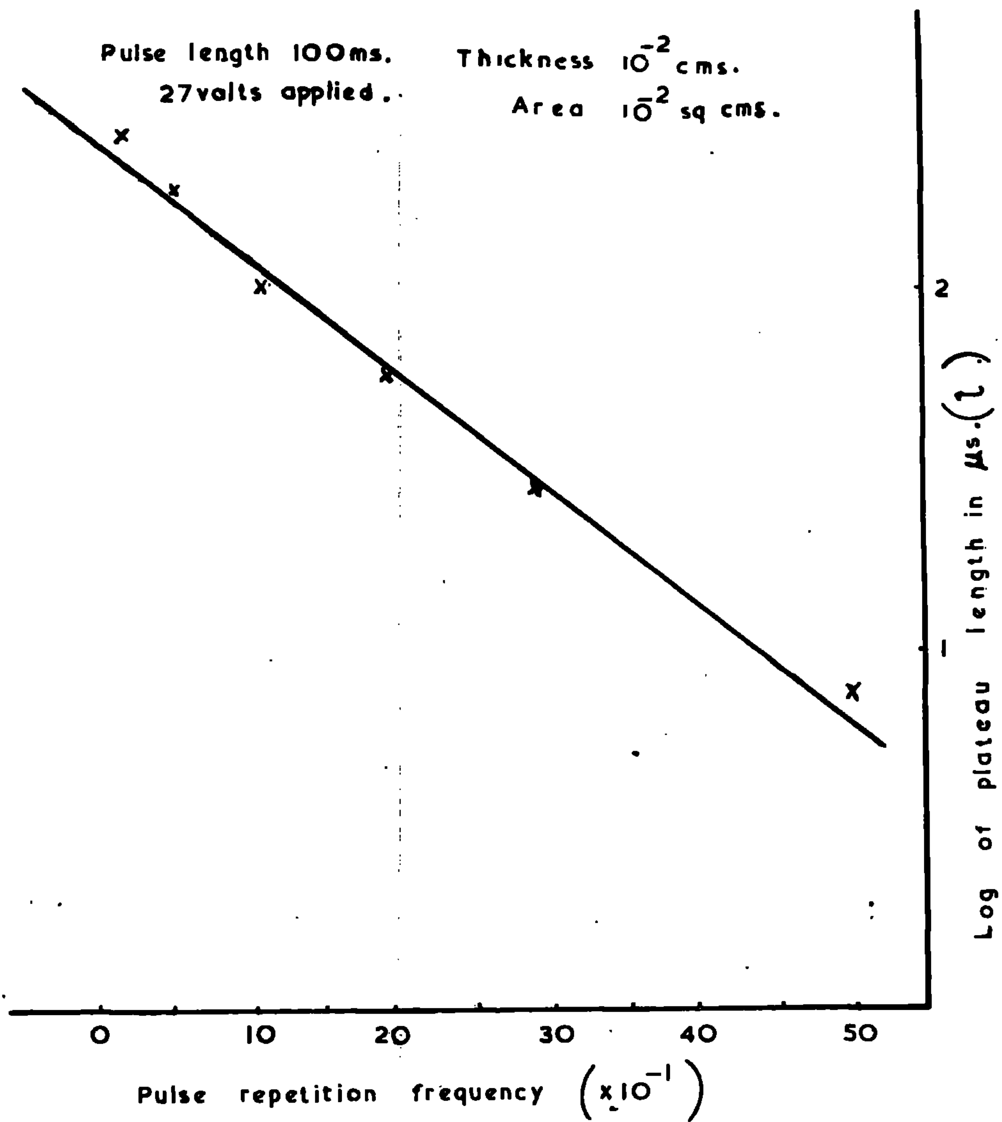

FIG. 5.4.4.

VARIATION OF PLATEAU LENGTH WITH P.R.F.

Once the crystal was exhibiting the behaviour of fig. 5.4.2. (d), this current pulse shape could be maintained at lower voltages, and at lower P.R.F.'s, than those required to establish the discontinuity.

The direct current and pulsed current characteristics have not been accurately determined for the same crystal. Preliminary measurements suggest that the transition, from Ohm's law to a cube law fig. 5.4.1., occurs at a similar voltage to the voltage causing the steep rise in current under direct current conditions (i.e. b, fig. 5.2.4).

5.5. Direct current luminescence

Under certain conditions steady voltages applied to cadmium sulphide crystals, maintained at the temperature of liquid air, lead to the emission of luminescence. Detailed observations were made by placing the crystal in a bath of liquid air and observing the luminescence under a microscope. The crystal was mounted on a microscope cover slip. The cover slip was held on a small block of polystyrene by two phosphor bronze spring wires which made the electrical connections to the crystal. These spring wires were, in turn, bolted to the polystyrene block. The steady voltages were derived from a battery. A series resistor (typically 10^3 ohms) was included in the circuit. The polystyrene block was inserted into a cavity cut out of expanded polystyrene. The cavity was filled with liquid air. This apparatus was

then placed on the stage of a microscope and the crystal observed with magnifications of up to 450 diameters. The experiment was carried out in a photographic darkroom.

Two distinct types of luminescence were observed.

(i) Green luminescence which was similar to edge emission (section 2.1.).

(ii) Green or red luminescence with properties suggesting high field phenomena.

(i) This luminescence was observed in crystals with indium cathodes, applied by heating in argon or by evaporation, and with anodes of graphite, gold, copper, silver or indium heated in argon. It was not observed in crystals with evaporated indium anodes. The voltages at which it was observed, for crystals with various contacts, are listed in fig. 5.5.1.

This luminescence was observed at 2.2 volts in one crystal with an indium cathode and a graphite anode. Crystals with graphite anodes were observed to luminesce readily at 3.0 volts or less. It was difficult to establish the exact voltage at which the green light was observed. On increasing the voltage from zero, the luminescence would steadily increase in intensity. No threshold could be determined accurately.

Microscopic observation of the luminescence failed to reveal any structure. It appeared as a faint glow which increased in intensity on raising the voltage until it could be readily seen with the naked eye. The faint glow appeared to come from beneath the contact.

CATHODE.	ANODE.	VOLTAGE.	THICKNESS x 10^{-3} cms.
* INDIUM	INDIUM	8·0	1·1
* "	"	10	2·6
* "	"	20	4·0
"	GRAPHITE	2·2	2·18
"	"	3·0	·6
* "	"	3·0	2·0
"	GOLD	8·0	1·33
"	"	30	8·0
"	"	20	4·0
* "	SILVER	9·0	12·0
* "	"	22	6·0
"	COPPER	9·0	~ 5·0

Indium contacts * were evaporated, the remainder were heated in argon.

No luminescence was observed with evaporated indium anodes.

FIG. 5.5.1.

SUMMARY OF THRESHOLD VOLTAGES FOR STEADY LUMINESCENCE.

Numerous attempts were made to determine the point of origin of the luminescence. These involved experiments with

(a) Semitransparent gold, silver or copper anodes.

(b) Contacts which were slightly displaced from each other, on opposite faces of the crystal.

(c) A top contact very much smaller than the bottom contact.

(d) An annular top contact to the crystal.

These techniques have not proved satisfactory for observation of the origin of this luminescence. Few crystals were mounted successfully. Either, the top spring contact broke the crystal if it was not adequately supported underneath by an anode, or the top contact was too small to locate with the spring contact. The high refractive index of cadmium sulphide also made detailed examination difficult and it was not possible, with the few crystals mounted, to determine the point of origin. Copper and silver did not make a good mechanical bond to the crystals when evaporated on to the surfaces.

A preliminary experiment has been carried out using a crystal with a silver anode and an indium cathode (heated in argon), to determine the point on the characteristic at which luminescence occurs. The apparatus used was that described in section 5.3. A photomultiplier with a Cs_3Sb cathode (RCA 931A) was used to detect the luminescence. Spurious voltages and insulation difficulties made the low current portion of the characteristic unreliable, and it is not presented here. However, the luminescence was first detected where the crystal entered

the negative resistance regime as illustrated in fig. 5.2.4 (c). The luminescence varied linearly with current according to

$$B = 2.0.10^{-3} I - 1.9.10^{-6} \qquad 5.5.(a)$$

where B is proportional to the intensity, and is the photo-multiplier current in microamps. I is the current through the crystal in milliamps. This result is expressed graphically in fig. 5.5.2., which shows the linear relation obtained.

This result is in agreement with qualitative observations made with crystals immersed in liquid air. In these experiments, luminescence was associated with a negative resistance phenomena. Luminescence was not observed in the absence of negative resistance. Extensive heat was not generated in crystals immersed in liquid air, as evidenced by the absence of appreciable boiling. The luminescence was stable over a period of hours.

(ii) The second type of luminescence referred to here as luminescence (II) could readily be distinguished from the luminescence (I) just described. Luminescence (II) originated at the high work function contact. It was localised in spots on the surface, and was observed at voltages which were an order of magnitude higher than those of fig. 5.5.1. At these voltages the crystals are generally very close to an irreversible breakdown. The point on the characteristic at which this type of luminescence is observed, however, has not been determined. Initially the luminescence originated from one spot on the surface, at the high work function contact. With

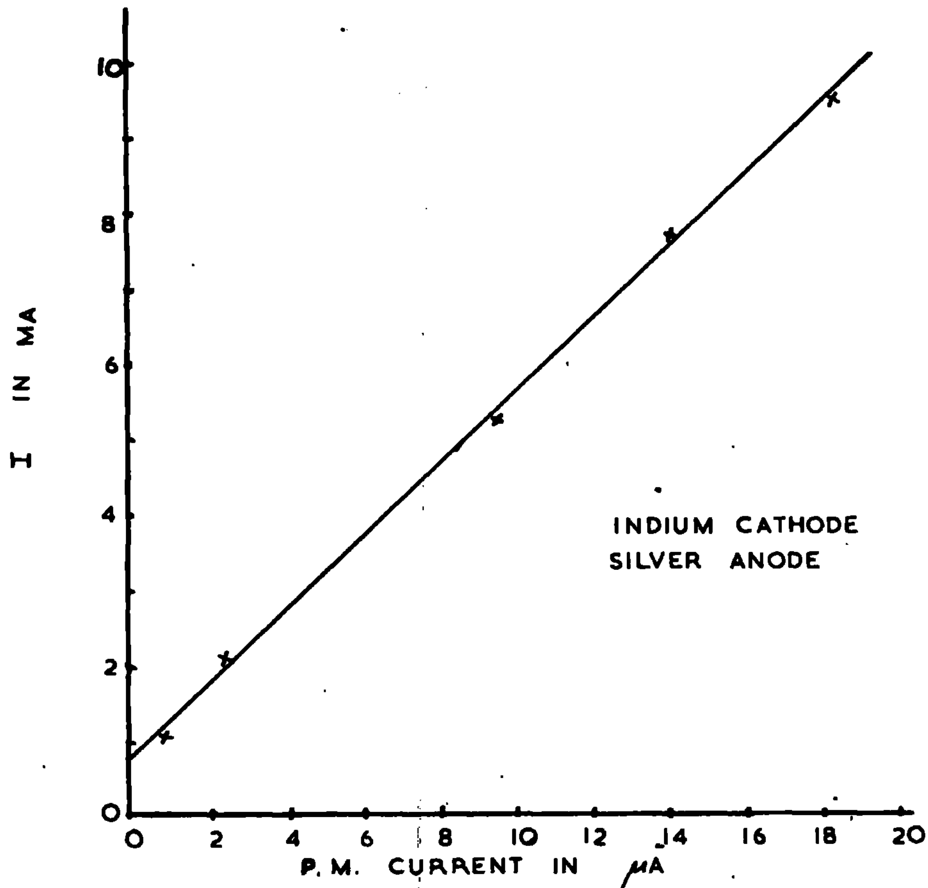

FIG 5. 5.2

INTENSITY OF LUMINESCENCE
VERSUS DIRECT CURRENT

increasing voltage more luminescent spots appeared. The number of such spots increased until the crystal was severely damaged. In contrast to the luminescence (I), the intensity of the emitted light was not steady but fluctuated rapidly. Excessive boiling of the liquid air indicated that considerable heat was being generated in the crystal. The colour of the luminescence varied from green to red. Many of the crystals displaying this luminescence suffered an irreversible change and some surface damage was generally observed.

5.6. Pulsed current luminescence

Green luminescence was also observed when pulsed voltages were applied to crystals maintained at the temperature of liquid air. Detailed observations under a microscope have not been made under pulsed conditions. Several features of this luminescence, however, have been determined. The measurements were obtained with the crystals immersed in liquid air. The photomultiplier was suspended over the crystal. Pulsed voltages were derived from a Nagard 5002 pulse generator and the resulting waveforms observed on a Tektronix 545A oscilloscope with a type CA plug-in unit.

The luminescence was not strictly in phase with the applied voltage. With applied voltages of the order of a few μs a delay of about 1μs was apparent before the onset of luminescence. Typical waveforms are illustrated in fig. 5.6.1. which show

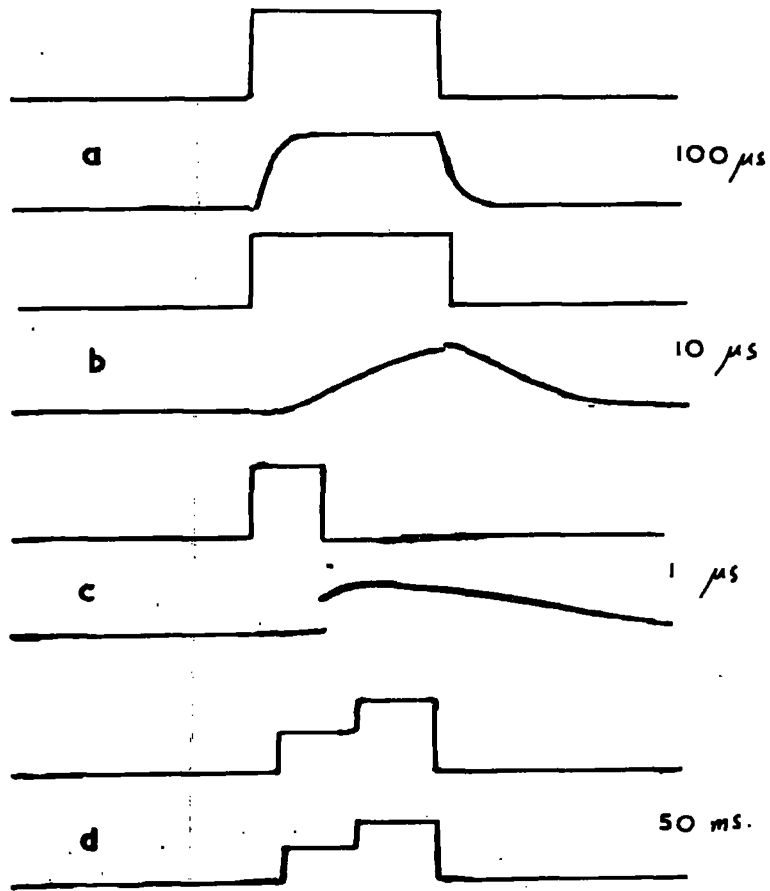

IN EACH PAIR: THE UPPER CURVE IS THE CURRENT PULSE
THE LOWER CURVE IS THE P.M. OUTPUT

FIG 5.6.1

PULSED LUMINESCENCE

the delay, and the rise and decay times of the luminescence. Fig. 5.6.1.(a) is for a pulse length of 100μs. The delay is just distinguishable. Fig. 5.6.1.(b) is for a pulse length of 10μs. The luminescence did not reach a steady value in this time, but the delay is more apparent. Fig. 5.6.1.(c) is for a pulse length of 1μs. No luminescence was observed until after the cessation of the current pulse. Further, the luminescence reached a maximum after the end of the current pulse, before decaying over a period of several microseconds.

The rise and decay time of the luminescence was of the order of 15μs. These times varied with the current passed through the crystal. The higher the current the faster the rise and decay time of the luminescence. Further measurements are required however to establish a quantitative relationship. The rise and decay times for five different currents are shown on fig. 5.6.2. The rise and decay times have not been measured for the 10μs and 1μs pulses which were not long enough to establish steady state luminescence.

The peak intensity of the luminescence varied linearly with current provided the pulse was long enough to establish steady luminescence. This is illustrated in fig. 5.6.2. It can be seen from fig. 5.6.2. that the maximum intensity of the luminescence is too low to fit the linear relation, when the applied pulse length is 10μs or 1μs.

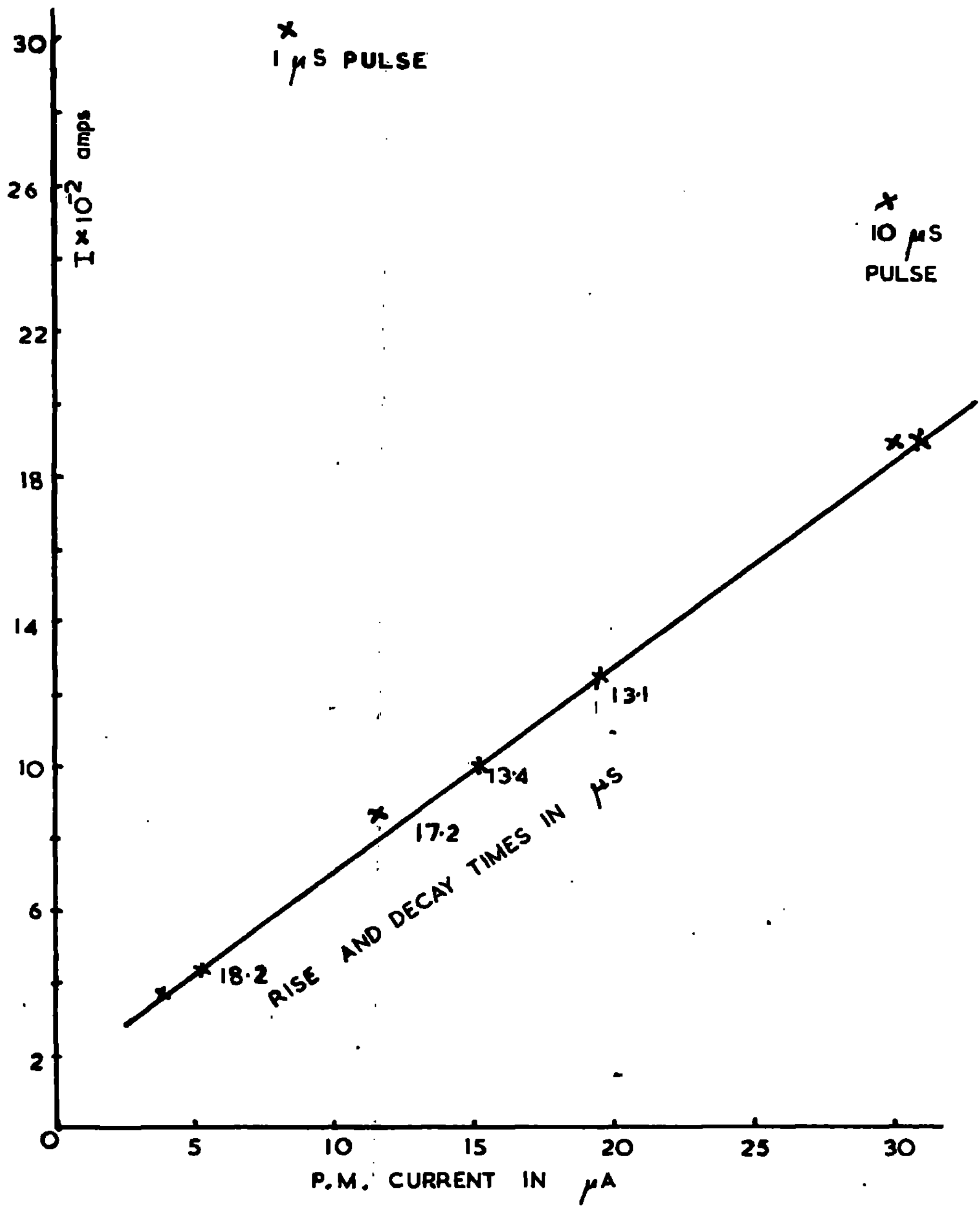

FIG 5.6.2.

INTENSITY OF LUMINESCENCE VERSUS PULSED CURRENT

The current discontinuity described in section 5.4 was also observed at liquid air temperatures. A similar discontinuity was observed in the intensity of the luminescence, co-incident with the current discontinuity. This phenomena is illustrated in fig. 5.6.1.(d). It has not been investigated.

When pulsed voltages were applied to crystals immersed in liquid air, a high pitched sound could sometimes be heard. The sound generally occurred when the crystal was displaying luminescence. The pitch varied with the pulse length and repetition frequency. The intensity increased with the current flowing through the crystal. Thus the intensity increased with decreasing voltage across the crystal, as the characteristic at this point was displaying negative resistance. The phenomena was attributed to a piezo-electric effect. No measurements were made of the phenomena.

The pulsed luminescence has been observed in crystals with contacts that showed the steady luminescence (I) described in section 5.5. For a summary of the contacts giving luminescence (I), refer to fig. 5.5.1. The waveforms illustrated (fig. 5.6.1.) and the measurements reported in this section, refer to a crystal with an indium cathode (heated in argon), and a graphite anode. Quantitative measurements have not been made with other contacts.

Chapter VI Discussion of results

6.1. Effect of contacts

Consider the upper Ohm's law region of fig. 5.2.3. Using equation 1.8 (k) [Ohm's law], the number of carriers/c.c. can be calculated on assuming a value for the mobility, $\mu = 250\ cm^2/volt.sec.$, say. Then

$$N_o = 9.0.10^{10} \text{ carriers/c.c.}$$

Substituting this value in equation 1.8 (b), the height of the barrier at the cathode is

$$\phi - \psi \approx 0.46eV$$

This value is of a similar order of magnitude to the condition for an Ohm's law region given in section 1.10.

Using equation 1.10 (e), which is the equation determining the transition from a square law to Ohm's law, the expected transition voltage is of the order of 1.2 volts for the crystal with the characteristic of fig. 5.2.3. (Assuming a dielectric constant of 11). This is a similar order of magnitude to the observed start of the Ohm's law region, which is at 8 volts.

The high degree of uncertainty in the thickness and area of contact makes it reasonable to assume that this is a genuine contact limitation. Thus, a limitation imposed by the contact obscures the expected square law characteristic.

The observation of luminescence described under (i) in section 5.5., can be used to infer some of the properties of the contacts. The luminescence can be due to one of two basic mechanisms; either an acceleration process or an injection process. In the acceleration process, electrons are excited from the valence band into the conduction band under impact with fast electrons. The recombination of the excited electrons, with the holes in the valence band via some recombination centre, produces the luminescence. For this process to be possible, the accelerated electrons have each to gain energy equal to the forbidden band gap. Calculations indicate that this process is only possible for fields $\gtrsim 10^6$ volts/cm. Curie (80) has reviewed the theories of electroluminescence. Typical field strengths were less than 10^4 volts/cm. for the observation of luminescence (I). In the injection process, electrons and holes are simultaneously injected from the cathode and anode respectively. Recombination of these injected electrons and holes produces the luminescence. The exact mechanism of the recombination process is, for the moment, unimportant. However, it is assumed, that the luminescence is due to the recombination of electrons and holes, in a similar manner to edge emission.

Observation of luminescence, with only 2.2 volts applied to a crystal, rules out the acceleration process. Electrons in this instance could gain a maximum energy of only 2.2eV,

which is insufficient for electronic excitation across the forbidden gap. (2.4eV). The observations of steady luminescence, which are summarised in fig. 5.5.1., also strongly support this conclusion. The voltages are such that the electron could gain the required minimum energy but are sufficiently low (between 3 and 30 volts) that this process is unlikely. The absence of distinct threshold voltages, the absence of irreversible changes in the crystals and the lack of structure in the luminescence, all support the conclusion that this is an injection phenomena.

The observations of injected luminescence in crystals with an indium anode, prepared by heating the crystal and indium in argon, indicate that this technique produces a hole injecting contact. Thus, indium anodes, prepared by this technique, do not make satisfactory hole blocking contacts for the observation of single carrier space charge limited currents. Conversely, the absence of luminescence in crystals with evaporated indium anodes, indicates that a contact prepared by evaporation is a good hole blocking contact.

Further work is required to determine whether or not evaporated indium contacts show the saturation effects discussed in section 6.1.

Graphite produced the most satisfactory hole injecting contact as evidenced by the consistently low voltages required for luminescence.

6.2. Direct current-voltage characteristics at room temperature

An analysis of the characteristics of fig. 5.2.3. and fig. 5.2.4. using Lampert's one carrier theory, (sections 3.1. to 3.3.), gives the following parameters for the two crystals, assuming $\mu = 250\ cm^2/volt.\ sec.$

Fig. 5.2.3.	Fig. 5.2.4.
$N_t = 2.0.10^{12}$ traps/cm^3	$N_t = 1.3.10^{13}$traps/cm^3
$V_1 = 0.5$ volts	$V_1 = 15$ volts
$E_t = 0.53$eV	$E_t = 0.70$eV
$\theta = 1.0.10^{-5}$	$\theta = 1.6.10^{-6}$

The transition voltages are modified by the factor θ (3.3.).

This analysis explains the characteristics within the limits of experimental error. The uncertainty in the thickness and area of contact could account for the discrepancy between the observed V_1 of fig. 5.2.4. (10·3volts) and the calculated value. N_t is the total trap density calculated from the voltage at which the current rises steeply. Equation 3.2.(d). V_1 is the transition voltage from Ohm's law to a square law, modified from Child's law for the trap free crystal by θ, [equation 3.3.(b)]. θ is obtained from the current range of the steep rise, and is the ratio of free to trapped carriers. E_t is the trap depth calculated from θ[equation 3.3.(a)].

The expected modified Child's law before the steep rise in current was not always observed.

However, as previously pointed out (section 2.6), the trap densities are lower than those that might reasonably be expected to occur in a crystal unless compensation processes are important. Further, Lampert's theory does not explain the negative resistance region of figs. 5.2.4. and 5.2.5.

The characteristic of fig. 5.2.4. does not permit an estimate of No. Thus, nothing can be learned about the cathode contact except that over the voltage range it remained ohmic. This in turn requires that the barrier height must be less than 0.5eV. The fact that at the highest voltages the curve remains three orders of magnitude below the theoretical Child's law, can be interpreted as due to shallow trapping levels which reduce the mobility of injected carriers.

The negative resistance regime of fig. 5.2.4. and fig. 5.2.5. can be interpreted in terms of double injection. According to suggestions put forward by Lampert (section 3.5.), the threshold voltage for two carrier current flow is given by

$$V_{th} = \frac{d^2}{2\mu_p \tau_{p\,low}}$$

where d is the thickness, μ_p the hole mobility and $\tau_{p\,low}$ the hole lifetime at low injection levels. Lampert pointed out

that the hole lifetime could increase by several orders of magnitude as the injection level increased.

From the characteristics we have

$$\mu_p \cdot \tau_p \text{ low} \approx 2.5.10^{-7} \text{ cm}^2/\text{volt.}$$

for both crystals.

Assuming a hole mobility (79)

$$\mu_p \approx 10 \text{ cm}^2/\text{volt.sec.}$$

the corresponding hole lifetime becomes

$$\tau_p \text{ low} \approx 2.5.10^{-8} \text{ secs.}$$

The characteristic of fig. 5.2.5. shows a large increase in current over the negative resistance region. Lampert predicted that there would only be a small increase in the current, of the order of five times (52). It was difficult to obtain closely spaced readings on the steeply rising portion of the characteristic, and this could account for the anomaly. The increase in current, over the negative resistance regime of the crystal whose characteristic is illustrated in fig. 5.2.4, was of the order of five.

The observation of injection luminescence at the start of the negative resistance regime indicates that this phenomena is due to double injection. The negative resistance regime can be interpreted as due to the increase in hole lifetime with increasing injection level. The square law of fig. 5.2.4. can be analysed using equation 3.5.(b). This

is the square law predicted by Rose and Lampert (50) for two carrier conduction where the space charge is neutralised. It is

$$J = e \tau \mu_n \mu_p \bar{n} \frac{V^2}{d^3} \qquad 3.5.(b)$$

where τ is the average lifetime.

Substituting in this equation, assuming $\mu_p = 10 cm^2$/volt. sec., and $\mu_n = 250\ cm^2$/volt.sec., we find $\tau \approx 10^{-5}$ secs. This indicates that the hole lifetime has increased by at least two orders of magnitude.

This analysis is only tentative, and more experimental data is required. However, from the observation of low threshold luminescence, in conjunction with a negative resistance regime, it seems reasonable to apply this analysis to the characteristic of fig. 5.2.4.

6.3. <u>The temperature variation of the direct current-voltage characteristics.</u>

To explain the anomalously low value of trap concentration computed from the traps filled limit, Allen (78) has considered a system with N_D shallow donors and N_A deep acceptors in the forbidden gap. He proposed that the acceptors compensated the donors during growth to produce high resistivity crystals. Assuming a mechanism of this nature, the electron concentration is given by

$$\bar{n} = \frac{N_C}{\chi} \exp \frac{E_A - E_C}{kT} \qquad 6.3.(a)$$

where $\chi \equiv \frac{N_A}{N_D} \gg 1$ and $E_C - E_A$ is the depth of the acceptor level below the conduction band.

The characteristics illustrated in fig. 5.3.2. have been analysed according to this model. A mobility of 210 cm^2/volt.sec. at 300°K was assumed, which varied according to $T^{-3/2}$. (20).

The number of carriers/c.c. was calculated from the ohmic portions of fig. 5.3.2. and a plot of log $\frac{\bar{n}}{T^{3/2}}$ against 1/T gave $E_C - E_A$ and χ, (from the slope and the intercept of the straight line respectively). This is illustrated in fig. 6.3.1.

The values obtained are $\chi \equiv \frac{N_A}{N_D} \simeq 240$

and $E_C - E_A \simeq 0.61$eV

A second method of evaluating the characteristics of fig. 5.3.2. is as follows. The voltage at which the characteristic departs from Ohm's law is related to the ratio of free to trapped carriers by equation 3.3.(b). Thus this ratio, θ, can be calculated for the eight different temperatures. Further θ is given by

$$\theta = \frac{N_C}{N_t} \exp \frac{E_t - E_C}{kT} \qquad 3.3.(a)$$

and a plot of log $\frac{\theta}{T^{3/2}}$ versus 1/T enables $E_C - E_T$ and N_t to be evaluated. This plot is illustrated in fig. 6.3.2.

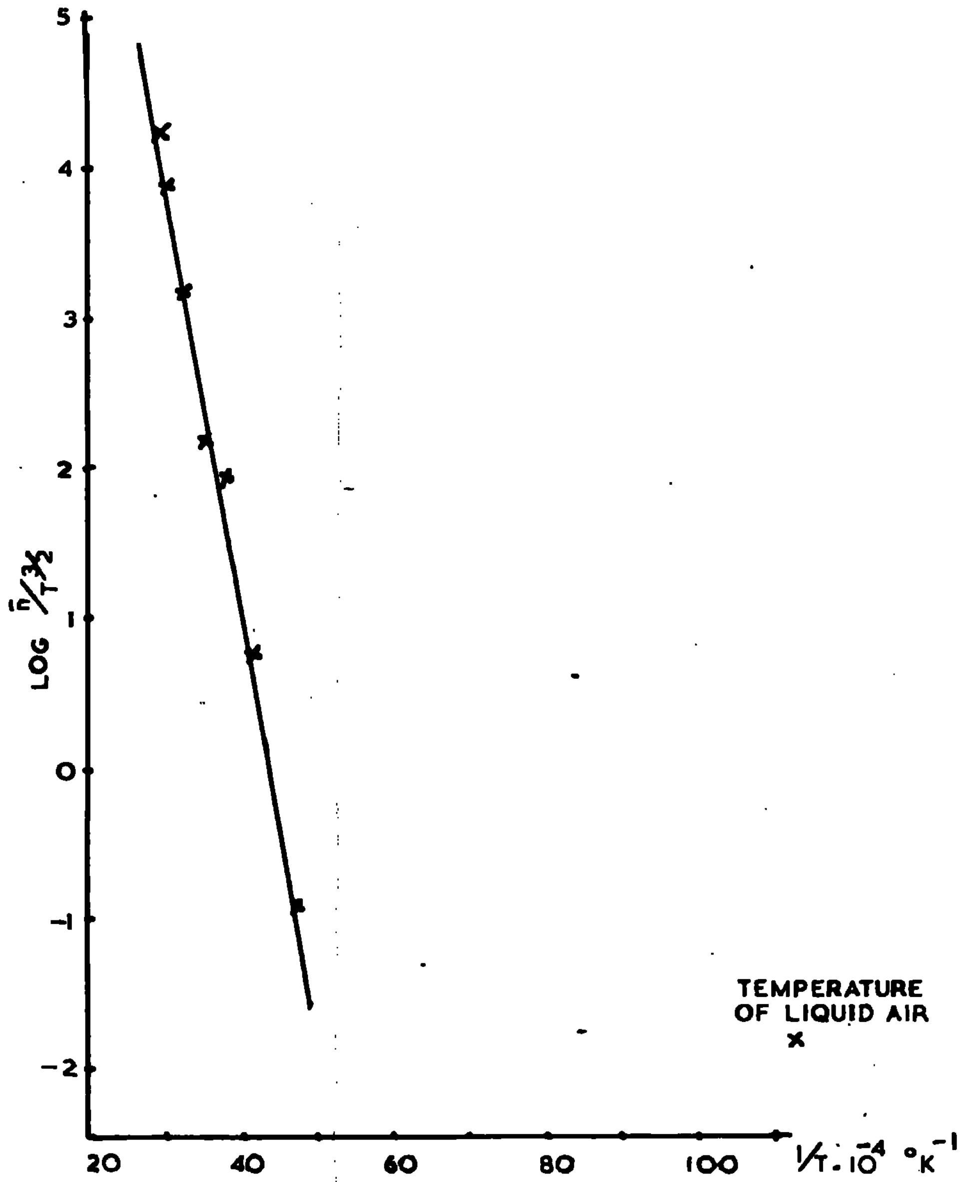

FIG 6.3.1

$\log \frac{\bar{n}}{T^{3/2}}$ VERSUS $1/T$

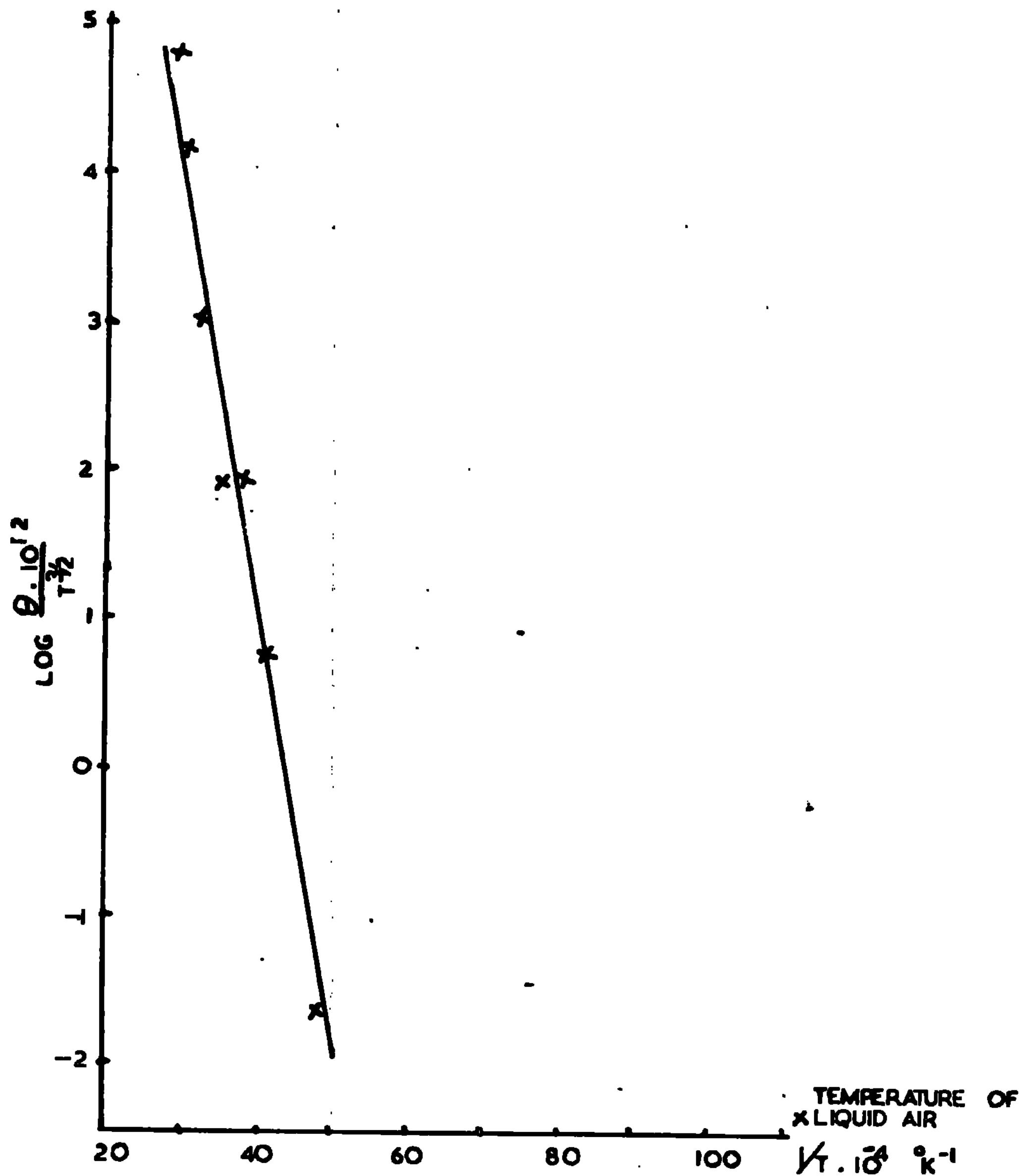

FIG 6.3.2

LOG $\frac{\theta}{T^{3/2}}$ VERSUS $1/T$

and gives for the trap depth and trap density

$$E_C - E_t \simeq 0.61 eV$$

$$N_t \simeq 2.4.10^{14} \text{ traps/c.c.}$$

Thus, on combining these two analyses, the number of donors is $N_D \simeq 10^{12}$ /c.c.

The transition from Ohm's law to a modified Child's law occurs when the excess injected carrier density, modified by the correction factor θ, equals the residual dark density $\bar{n}$. In a two level system, the ratio of the number of free carriers to the number of trapped carriers is approximately $\theta = \frac{\bar{n}}{N_D}$ since all the electrons from the N_D donors may be taken as trapped in the N_A acceptors (i.e. $\bar{n} \ll N_D$). Substituting $\theta = \frac{\bar{n}}{N_D}$ in the plot of fig. 6.3.2., where $N_D = 10^{12}$, should give the plot illustrated in fig. 6.3.1. Comparison of the two straight lines shows that this argument is correct, the same straight line is obtained on making this substitution. (Fig. 6.3.2. is plotted as $\theta \times 10^{12}$ versus 1/T for convenience).

From a measurement of the traps filled limit for this crystal, the trap density according to Lampert's one carrier theory is

$$N_t = 3.0.10^{13} \text{ traps/c.c.}$$

Calculations based on the temperature variation of the characteristic give a more realistic estimate of the total trap density N_t, or N_A, than do measurements based on the traps filled limit theory. However, the reason for the steep

rise in current requires explanation. Two alternatives to a traps filled limit mechanism exist.

(i) The space charge of trapped carriers is removed by hole injection. Thus the steep rise is due to trap emptying by recombination of the trapped electrons with injected holes. There is no evidence for this with evaporated indium contacts. The recombination, however, could take place without luminescent emission.

(ii) The steep rise in current is due to removal of the trapped space charge by impact ionisation or by field ionisation of the carriers from traps. Assuming a two level system, the current range of the steep rise would be given by $\frac{1}{\theta} = \frac{N_D}{\bar{n}}$. Thus, an explanation of the steep rise in terms of ionisation of trapped donors, would give the same experimental fit as the one carrier traps filled limit theory. The voltage required for the ionisation of trapped donors would not be related to the total trap density. In view of the satisfactory estimates derived for the total trap density, and for the ratio of donors to acceptors, it seems probable that this mechanism (i.e. Impact ionisation or field ionisation of trapped donors) is responsible for the steep reversible rise in current.

The measurements taken at the temperature of liquid air, plotted in fig. 6.3.1. and fig. 6.3.2., do not lie on the experimental straight line. The currents that were measured, fig. 5.3.2., were far too high. This is attributed to leakage

of current across the surface of the crystal. The effects of surface conduction would be greatest at the lowest temperature. A general criticism of the low current measurements is that no precautions were taken to reduce surface leakage.

6.4. <u>Current-voltage characteristics using pulsed fields.</u>

The observation of luminescence (at the temperature of liquid air) with low threshold voltages in crystals with indium anodes applied by heating in argon, suggests that a contact of this nature will permit hole injection. The measurements of section 5.4. will therefore be interpreted exclusively in terms of double injection. The characteristic of fig. 5.4.1. can be analysed using equation 3.5.(a). This is the equation derived by Lampert and Rose (51) assuming a constant lifetime for electrons and holes. Lampert and Rose predicted that this cube law would be followed if the transit time is less than the relaxation time (section 3.5.). The absence of a square law regime in the characteristic requires that the thermal equilibrium densities of holes and electrons are approximately equal(51).

Assuming $\mu_n \approx 250$ and $\mu_p \approx 10$ cm^2/volt.sec., the common recombination time calculated from fig. 5.4.1. using equation 3.5.(a) is

$$\tau \approx 2.0.10^{-8} \text{ seconds.}$$

Considering the Ohm's law to a cube law transition, the

transit time calculated from the transition voltage, which was 20 volts, is

$$\tau_L \approx 2.0.10^{-8} \text{ seconds}$$

(The transit time is given by $\tau_L = \frac{d^2}{V\mu_n}$).

Thus, the condition that the transit time should be less than the common lifetime is fulfilled for the cube law regime of fig. 5.4.1.

The reason for the depression in the current pulse illustrated in fig. 5.4.2.(b) is not yet clear. It is possible that the filling of fast trapping states could be invoked to explain the phenomena. Similarly, the empirical relation for the decay, equation 5.4.(a), cannot be explained. Several trapping levels may be responsible for this decay. An alternative explanation for the depression observed in the current pulse might be found in terms of electron-hole recombination.

The constants of equations 5.4.(b) (c) have been calculated from figs. 5.4.3. and 5.4.4. They are

$$\alpha \approx 3.10^{4} \qquad \beta \approx 2.2. \text{ (for a 10ms pulse).}$$
$$\gamma \approx 3.10^{-4} \qquad \delta \approx 0.5. \text{ (for a 100ms pulse).}$$

A possible explanation of the observed discontinuities might be obtained if they are related to impact ionisation of trapped carriers. Accelerated carriers remove trapped electrons and permit higher currents to flow. The P.R.F.

and pulse length could then be related to the residual number of carriers available in the crystal before the application of a pulse.

Alternatively it may be that a consideration of contact controlled response times (3.7.), could clarify the situation.

Further results are required before any firm conclusions can be drawn.

6.5. Analysis of direct current luminescence

From the observation of steady luminescence at low voltages the existence of hole injection can be deduced. This has been considered in section 6.1. The origin of the irregular luminescence, (described under (ii), section 5.5), can be attributed to high field phenomena. For example, an avalanche multiplication of carriers, (42,43). This would lead to the creation of electron-hole pairs in the crystal, their recombination producing the luminescence.

The linear variation of the low voltage luminescence (equation 5.5.(a)) suggests a monomolecular recombination process. Approximate first order recombination kinetics would hold if the majority carrier density were large, and it could appear to be constant. If it is assumed that recombination takes place with free holes combining with trapped electrons(27) then a large fraction of injected electrons must be trapped. Further, the density of trapped electrons must remain constant in the face of recombination. This implies rapid trapping of

injected electrons.

Further measurements are required to determine the spectral distribution of the low voltage luminescence.

It has already been pointed out in section 6.2., that the coincidence of negative resistance and luminescence strongly indicates that hole injection is responsible for the former phenomena.

6.6. Pulsed current luminescence

The luminescence is assumed to be injection luminescence. The delay observed before the onset of luminescence (fig. 5.6.1.(c)) can be interpreted as the time required for injected holes to drift across the crystal and recombine with electrons trapped near the cathode. For this to be possible, the lifetime of injected holes must be greater than their transit time across the crystal. The delay was 1μsec., with 10 volts applied across 10^{-2}cms of crystal.

Thus, taking this delay as the transit time, the hole mobility would be

$$\mu_p \approx 10 \text{ cm}^2/\text{volt.sec.}$$

The lifetime of the holes must be of the order of 10^{-6} seconds. This is much longer than the value estimated in the previous section, and the value estimated in section 6.2. from the negative resistance phenomena. However, it was also shown in section 6.2., that the hole lifetime might

be expected to increase by at least two orders of magnitude at high injection levels. Thus, the removal of trapped electrons by recombination, could lead to the required lifetime of the order of 10^{-6} secs. The rise and decay times of the luminescence, indicated on fig. 5.6.2., are of the order of several microseconds, indicating a similar order of magnitude for the hole lifetime. The decrease in these rise and decay times with increasing current through the crystal, can be interpreted as faster recombination at higher injection levels, as opposed to a variation in lifetime with injection level due to the removal of trapped electrons. The observation of a maximum in the luminescence after the cessation of the current pulse supports this hypothesis (fig. 5.6.1.(c)). Thus it is concluded that the sudden onset of luminescence some microseconds after the application of the voltage indicates the arrival of a pulse of holes at the cathode. The long tail on the luminescence indicates a hole lifetime of the order of several microseconds.

It was pointed out in the last section that a constant number of trapped electrons, recombining with free holes, would give a linear luminescence intensity versus current relationship. This agrees with the conclusions of this section, and the linear relations observed, under direct current and pulsed current, are attributed to this mechanism. The maximum of the luminescence observed with pulses of 10μs

and 1μs was too low to fit the linear relation which held for longer pulses. This indicates that the lifetime of the holes is of the order of 10μs, since for the 10μs pulse, the intensity observed was about $\frac{2}{3}$ the expected value.

Possible explanations for the observed phenomena, in terms of a contact controlled response, or the time required for significant recombination, do not explain the absence of luminescence for 1μs at the start of the current pulse.

The observation of a discontinuity in the luminescence (fig. 5.6.1.(d)) coincident with the current discontinuity is interpreted as more holes reaching the cathode. The cause of the current discontinuity, however, is not clear. Rapid trapping of electrons near the cathode would explain the depression observed in current pulses described in section 5.4. (fig. 5.4.2.(b)).

Further investigation of conduction and luminescence processes under pulsed field conditions is necessary.

Chapter VII Conclusions

7.1. Crystal growth

Single crystals which are satisfactory for investigating space charge effects and double injection phenomena can be grown by a sublimation technique. Further work is required to determine the effects of oxygen on the crystal growth and crystal properties. It is necessary to exclude oxygen to grow suitable single crystals. The mechanism of crystal growth is not clear.

7.2. Contact to cadmium sulphide

Electron injecting contacts can be made to cadmium sulphide by evaporating indium on to the crystal. Soldering or diffusion techniques are not satisfactory.

Hole injecting contacts can be made to cadmium sulphide using a variety of high work function materials. Graphite was the most satisfactory of the contacts investigated.

Hole blocking contacts can be made by evaporating indium on to the crystal. Diffused indium contacts formed hole injecting contacts.

7.3. Single carrier space charge limited conduction

Measurement of the current-voltage characteristic of a crystal at different temperatures is a satisfactory technique for determining trap densities. The trap densities determined by this technique are more realistic than those calculated from the steep rise in current, on assuming

that this is due to a traps filled limit behaviour. The steep rise in current can be associated with the ionisation of trapped carriers. However, the mechanism involved in the ionisation of trapped carriers is not clear. One suggested mechanism is an impact ionisation process.

7.4. Two carrier space charge limited conduction

Two carrier space charge limited conduction provides a satisfactory explanation for a number of experimentally observed phenomena. From the luminescence measurements it is concluded that hole injection occurs with suitable contacts, and that the lifetime of holes can increase by orders of magnitude at high injection levels. Further investigation is required of two carrier space charge limited conduction under pulsed fields.

REFERENCES

(1) (a) C. Kittel. Introduction to Solid State Physics Wiley, 2nd Ed. 1959.

(b) N. Cusack. The Electrical and Magnetic Properties of Solids. Longmans 1958.

(c) F. Seitz. A Modern Theory of Solids. McGraw-Hill 1940.

(2) N.F. Mott and R.W. Gurney. Electronic Processes in Ionic Crystals. O.U.P. 2nd Ed. 1940, pp. 168-173.

(3) W. Shockley and R.C. Prim. Phys. Rev. 90, 753 (1953).

(4) G.T. Wright. Proc. Inst. E. E. 106B 17. 915 (1959).

(5) M.A. Lampert. Phys. Rev. 103, 1648 (1956).

(6) R.H. Bube. Photoconductivity of Solids. p.38 ff. Wiley 1960.

(7) J. Lambe, C.C. Klick. Electronic Processes in CdS. Progress in Semiconductors Vol. 3. 185 Heywood, London (1958).

(8) R. Frerichs. Phys. Rev. 72, 594 (1947)

(9) Czyzak, Craig, McCain and Reynolds. J.A.P. 23, 932 (1952)

(10) M.E. Bishop, S.H. Liebson. J.A.P. 24, 660 (1953).

(11) E.S. Rittner, J.H. Schulman. J. Phys. Chem. 47, 537 (1943)

(12) Kroger, Vink and van der Boomgaard. Z. Phys. Chem. B.203, 1 (1954).

(13) D.A. Jenny and R.H. Bube. Phys. Rev. 96, 1190 (1954)

(14) Kroger, Vink and Volger. Phil. Res. Rep. 10, 39, (1955)

(15) R.H. Bube. J. Chem. Phys. 23, 18 (1955)

R.H. Bube. J. Phys. Chem. Solids. 1, 234 (1957)

R.H. Bube. Phys. Rev. 99, 1105 (1955)

(16) R.H. Bube and S.M. Thomsen. J. Chem. Phys. 23, 15 (1955)

(17) C.C. Klick. Phys. Rev. 89, 274 (1953)

(18) D.C. Reynolds, R.C. Allen and C.C. Reynolds. J. Opt. Soc. Amer. 45, 136 (1955).

(19) Sommers, Berry and Sochard. Phys. Rev. 101. 987 (1956)

(20) F.A. Kroger, H.J. Vink and J. Volger. Physica 20, 1095 (1954)

(21) P.J. van Heerden. Phys. Rev. 106 468 (1957)

(22) In A. Shuba. J. Tech. Phys. Moscow. 26, 1129-1134 (1956)

(23) J.J. Scheer and J. van Laar. Phil. Res. Rep. 16, 323-328 (1961).

(24) R.W. Smith. Phys. Rev. 97. 1525 (1955)

(25) F.A. Kroger. Physica 7, 1 (1940)

(26) F.A. Kroger and H.J.G. Meyer. Physica 20, 1149 (1954)

(27) Lambe, Klick and Dexter. Physics Rev. 103, 1715 (1956)

(28) W.M. Buttler, W. Muscheid. Ann. Physik. 14, 215 (1954)

(29) W.M. Buttler, W. Muscheid. Ann. Physik. 15, 82 (1954)

(30) J. Fassbender. Z. Phys. 145. 307, 1956.

(31) G.F. Alfrey and I. Cooke. Proc. Phys. Soc. 70B 1096 (1957)

(32) F.A. Kroger, G. Diemer and H.A. Klasens. Phys. Rev. 103, 279 (1956)

(33) R.W. Smith. Phys. Rev. 105 900 (1957)

(34) (a) W. Ruppel. Helv. Phys. Acta. 31, 311 (1958)

(b) Proc. International Conference on Semi-conductors, Prague 1960.

(35) G.T. Wright. Nature 182, 1296 (1958)

(36) G.C. Dacey. Phys. Rev. 90, 759 (1953)

(37) R.W. Smith and A. Rose. Phys. Rev. 97, 1531 (1955)

(38) A. Rose. Phys. Rev. 97, 1538 (1955)

(39) A. Rose, M.A. Lampert, R.W. Smith. J. Phys. Chem. Solids 8, 464 (1959).

(40) K.W. Boer, U. Kummel. Z. Naturforsch 9 a 177 (1954)

(41) K.W. Boer, U. Kummel. Z. Phys. Chem. 200 193 (1952)

(42) K.W. Boer, U. Kummel, R. Rampe. Z. Phys. Chem. 200 180 (1950)

(43) G. Diemer. Philips. Res. Rep. 9 109 (1954)

(44) G.T. Wright. Proc. Inst. Elec. Eng. 106B 2928 (1959)

(45) W. Ruppel. J. Phys. Chem. Solids 22 199 (1961)

(46) R.H. Bube. J.A.P. 33, 1733 (1962)

(47) S.M. Skinner. J.A.P. 26, 498 (1955)

(48) G.H. Suits. J.A.P. 28, 454 (1957)

(49) R.H. Parmenter, W. Ruppel. J.A.P. 30, 1548 (1959)

(50) M.A. Lampert. R.C.A. Rev. 20 682 (1959)

(51) M.A. Lampert, A. Rose. Phys. Rev. 121, 26, (1960)

(52) M.A. Lampert. J. Phys. Chem. Solids. 22, 189 (1961)

(53) R.W. Smith. R.C.A. Rev. 12, 350 (1951)

(54) I. Broser, R. Warminsky. Ann. Phys. Lpz. 7, 289 (1950)

(55) A. Rose. M.A. Lampert. R.C.A. Rev. 20, 57, (1959)

(56) A. Rose. M.A. Lampert. Phys. Rev. 113 1227 (1959)

(57) R.W. Redington. J.A.P. 29, 189, 1958
Phys. Rev. 115, 894, 1959.

(58) R.W. Smith. R.C.A. Rev. 20, 69 (1959)

(59) H.B. DeVore. R.C.A. Rev. 20, 79 (1959)

(60) R.H. Bube, L.A. Barton. R.C.A. Rev. 20 564 (1959)

(61) M.A. Lampert. Phys. Rev. 125, 1, 126 (1962).

(62) R. Frerichs. Naturwiss, 33, 281 (1946)

(63) F. Schossberger. J. Electrochem Soc. 102, 22, (1955)

(64) L. Herforth. J. Krumbiegel, Naturwiss. 40, 270, (1953)

(65) R.H. Bube, S.M. Thomsen. J. Chem. Phys. 23, 15, (1955)

(66) R.J. Miller, C.H. Bachman, J.A.P. 29, 1277, (1958)

(67) L.E. Hollander. Rev. Sci. Inst. 28, 322, (1957)

(68) Reynolds, Czyzack, Allen, Reynolds. J. Opt. Soc. Am. 45, 136, (1955). J. Opt. Soc. Am. 44, 864 (1954)

(69) Reynolds, Czyzack, Baker, Greene. J. Chem. Phys. 29, 1375 (1958)

(70) D.C. Reynolds, L.C. Greene. J.A.P. 29, 559 (1958)

(71) W.W. Piper, S.J. Polich. J.A.P. 32, 1278 (1961)

(72) P.D. Fochs. J.A.P. 31, 1733 (1960)

(73) J.M. Stanley. J. Chem. Phys. 24, 1279 (1956)

(74) R. Nitsche. J. Phys. Chem. Solids. 17, 163, (1960)

(75) Nitsche, Bölsterli, Lichtensteiger. J. Phys. Chem. Solids. 21, 199 (1961)

(76) J. Woods. B.J.A.P. 10, 529 (1959)

(77) R.H. Bube. J. Chem. Phys. 21, 1409 (1953)

(78) J.W. Allen. Nature 187, 403 (1960)

(79) W.E. Spear, J. Mort. Phys. Rev. Letters. 8, 314 (1962)

(80) D. Curie. Prog. in Semiconductors Vol. 2. 251. Heywood (1957).